"Experimental study the cold dense baryon matter in high p_T processes"

S.S. Shimanskiy
(JINR, Dubna)

The plan

1. The Cold Dense Baryon Matter – where it is?
2. The Ace in Our Hands – cumulative processes.
3. Why the high p_T?
4. FLINT, SPIN and FODS

The Cold Dense Baryonic Matter – where it is?

An example of useless compressed baryonic matter

How well we know the strong NN-interaction and structure of the nuclear matter (nowadays situation) ?

Let us look at the nucleon-nucleon interaction:

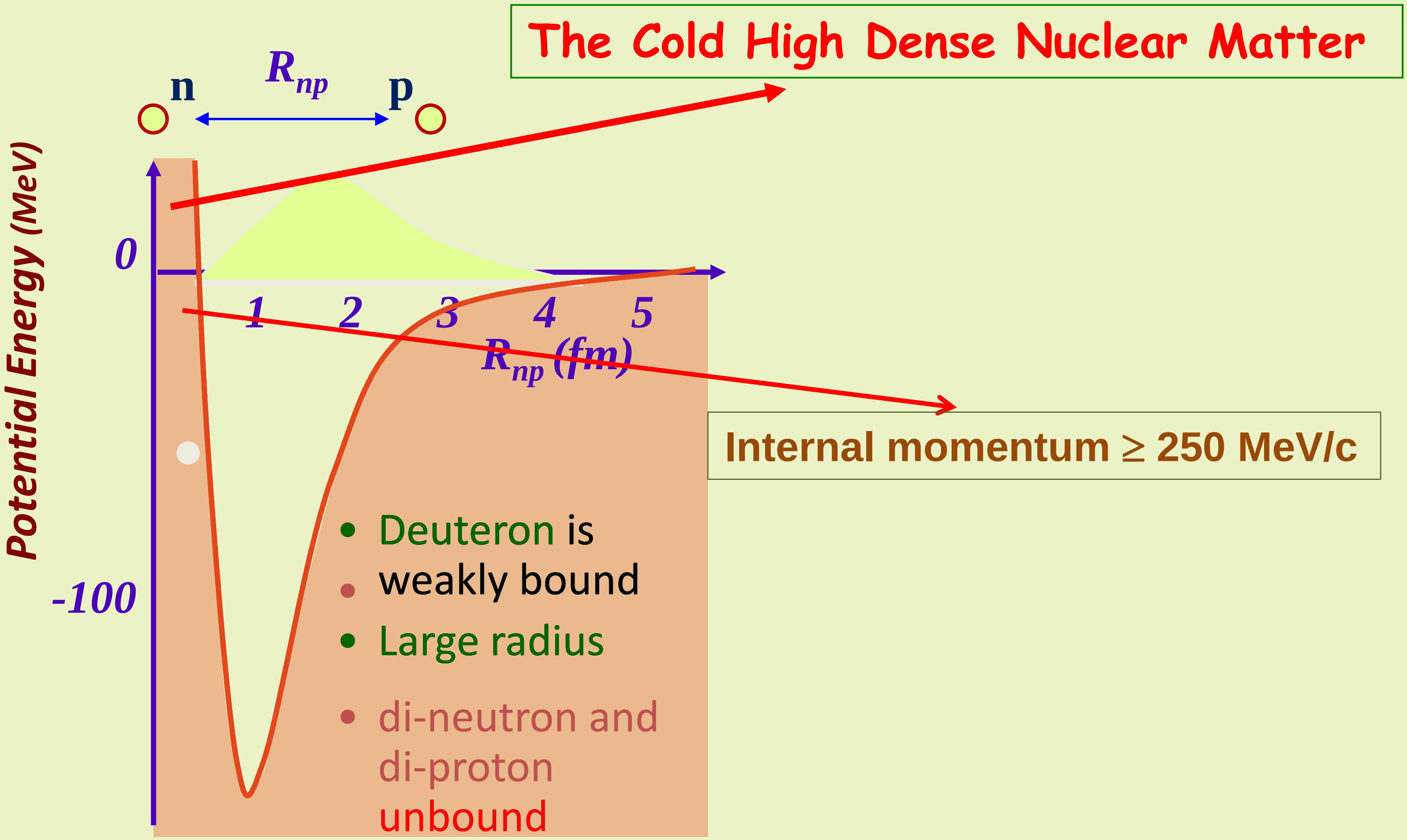

DEUTERON STATIC PROPERTIES FROM NN-POTENTIALS

Таблица 1: Статические свойства дейтрона

	$E_D(MeV)$	$P_D(\%)$	$< r_D^2 >^{1/2}\ (fm)$	$Q(fm^2)$	$\eta = \frac{A_D}{A_S}$	$f^2_{\pi NN}$	$\mu_D(n.m)$
Exp.	2.224579(9)	—	1.9560(68)	0.2859(3)	0.0271(4)	0.0776(9)	0.857406(1)
MU	2.2246	6.78	1.9611	0.2860	0.0271	0.07745	0.843
Paris	2.2250	5.77	1.9716	0.2789	0.0261	0.078	0.853
RHC	2.2246	6.50	1.9602	0.2770	0.0259	0.0757	0.840
RSC	2.2246	6.47	1.9569	0.2796	0.0262	0.0757	0.843
Bonn	2.225	4.58	1.86	0.2856	0.0267	—	—

Table 1: Deuteron properties in the dressed bag model.

Model	E_d(MeV)	$P_D(\%)$	r_m(fm)	$Q_d(\text{fm}^2)$	$\mu_d\ (\mu_N)$	$A_S(\text{fm}^{-1/2})$	$\eta(D/S)$
RSC	2.22461	6.47	1.957	0.2796	0.8429	0.8776	0.0262
Moscow 99	2.22452	5.52	1.966	0.2722	0.8483	0.8844	0.0255
Bonn 2001	2.224575	4.85	1.966	0.270	0.8521	0.8846	0.0256
DBM (1) $P_{\text{in}} = 3.66\%$	2.22454	5.22	1.9715	0.2754	0.8548	0.8864	0.0259
DBM (2) $P_{\text{in}} = 2.5\%$	2.22459	5.31	1.970	0.2768	0.8538	0.8866	0.0263
experiment	2.224575		1.971	0.2859	0.8574	0.8846	0.0263

RHIC Physics: 3 Lectures*

Larry McLerran
Physics Department PO Box 5000 Brookhaven National Laboratory Upton, NY 11973 USA

September 13, 2003

+ CERN Yellow Report 2007-005, p.75

The Evolving QCD Phase Transition

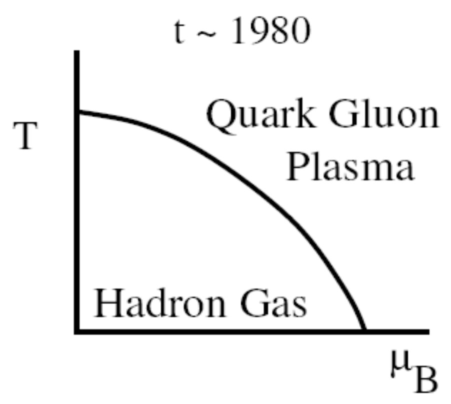

Critical Temperature 150 - 200 MeV ($\mu_B = 0$)
Critical Density 1/2-2 Baryons/Fm^3 ($T = 0$)

SPS Time (CERN)

RHIC Time(BNL)

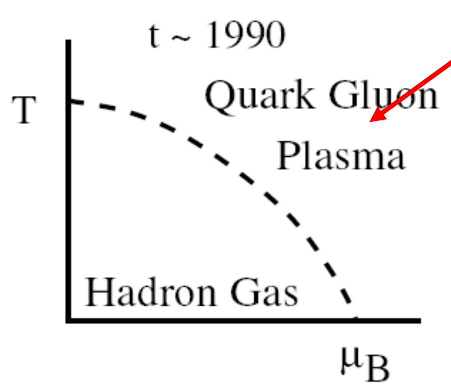

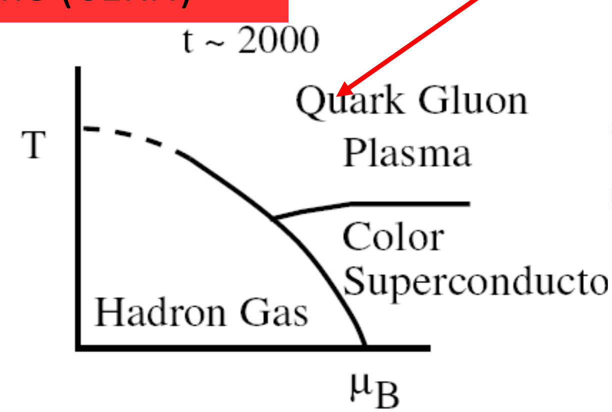

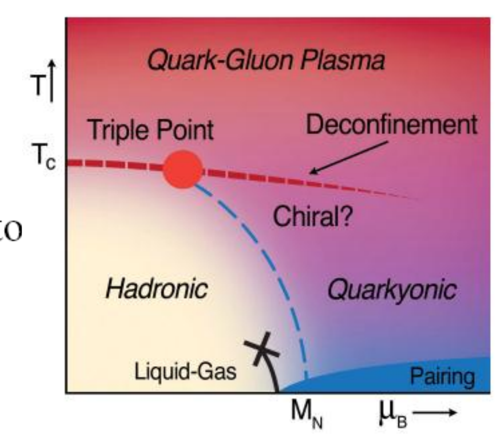

Figure 4: A phase diagram for QCD collisions.

Strangeness in Neutron Stars

FRIDOLIN WEBER,* ALEXANDER HO,† RODRIGO P. NEGREIROS,‡
PHILIP ROSENFIELD§

H ~ 10^{17} Gs

E~ 10^{19} V/cm

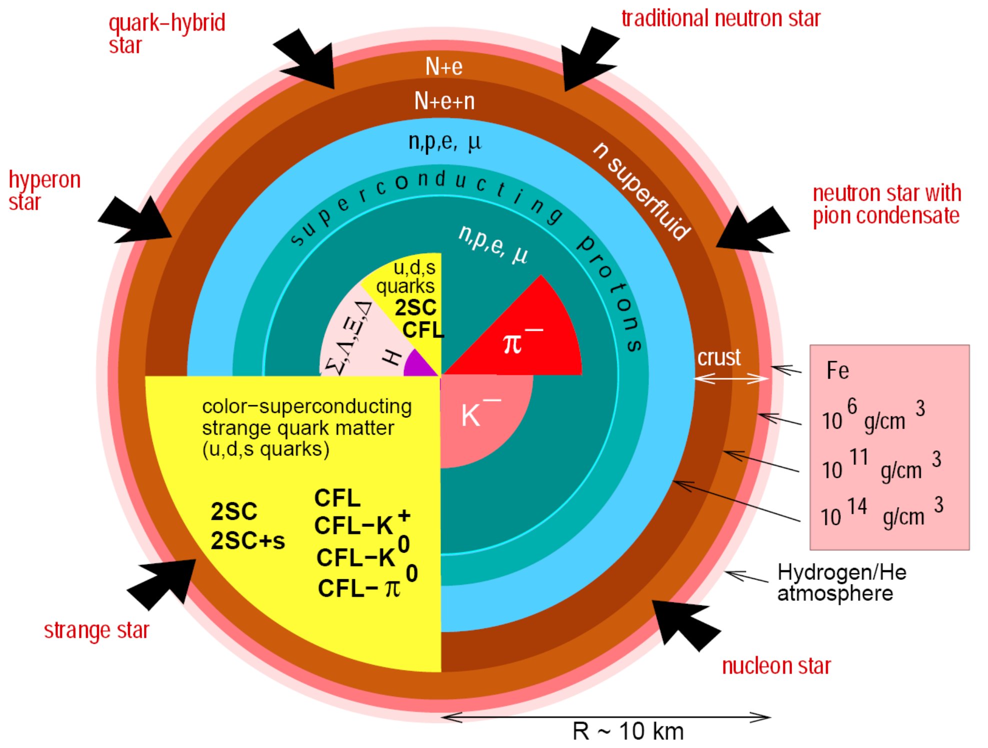

Fig. 1. Competing structures and novel phases of subatomic matter predicted by theory to make their appearances in the cores ($R \lesssim 8$ km) of neutron stars[4].

K. Rajagopal and F. Wilczek, *T*
of Particle Physics / Handbook
M. Alford, Ann. Rev. Nucl. Par

significant range of chemical potentials and strange quark masses[51]. If the strange quark mass is heavy enough to be ignored, then up and down quarks may pair in the two-flavor superconducting (2SC) phase. Other possible condensation patters

color–superconducting strange quark matter (u,d,s quarks)

«ФИЗИКА ЭЛЕМЕНТАРНЫХ ЧАСТИЦ И АТОМНОГО ЯДРА»
1997, ТОМ 28, ВЫП.1

THERMODYNAMICS OF STRONG INTERACTIONS

V.I.Yukalov, E.P.Yukalova

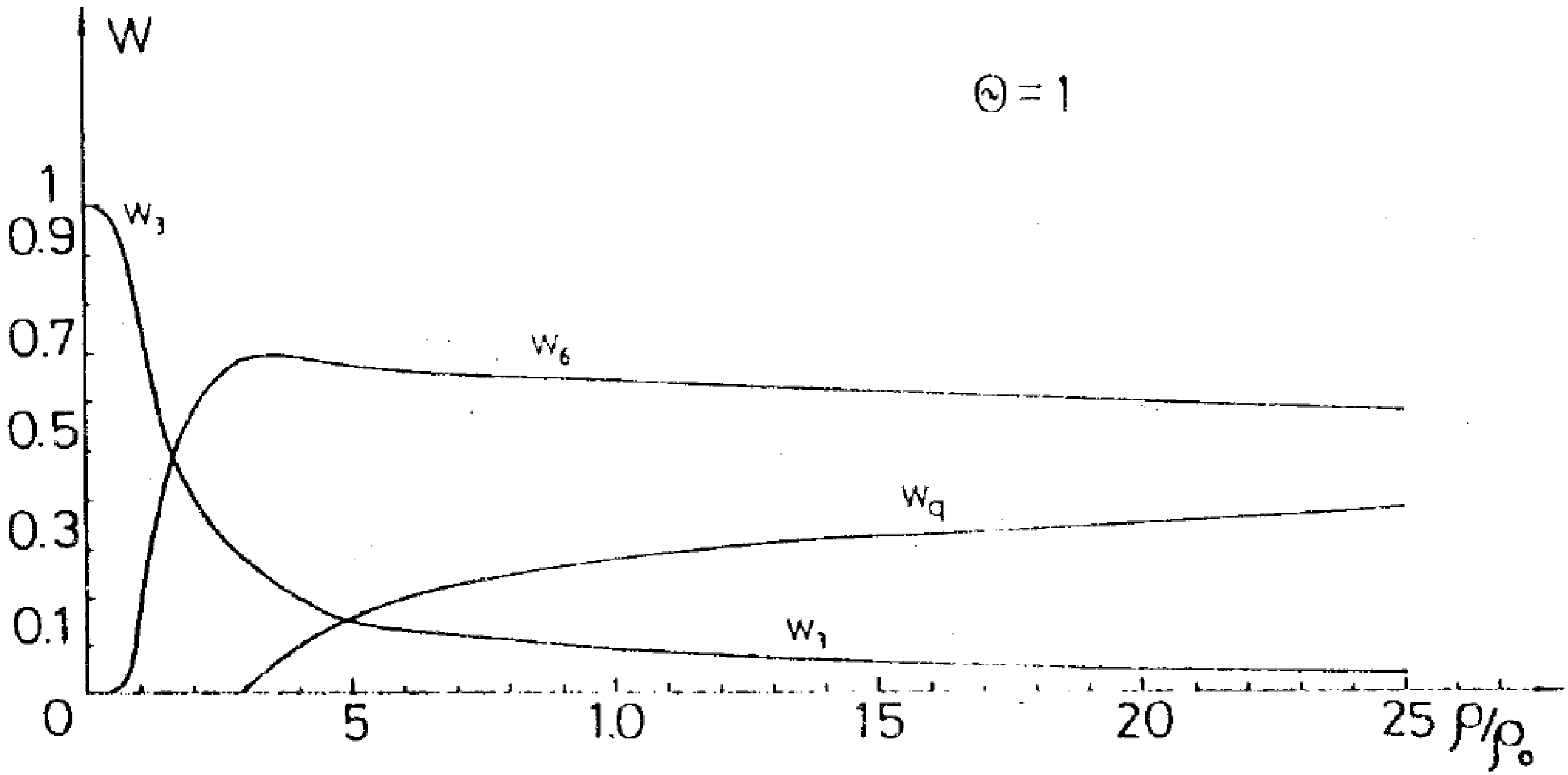

Fig.6. Nucleon, 6*q*–cluster, and unbound quark probabilities as functions of the relative density at Θ = 0

Structure of Matter

F. Close

Two ways that structure is revealed:

$$A^* \rightarrow A + \gamma$$

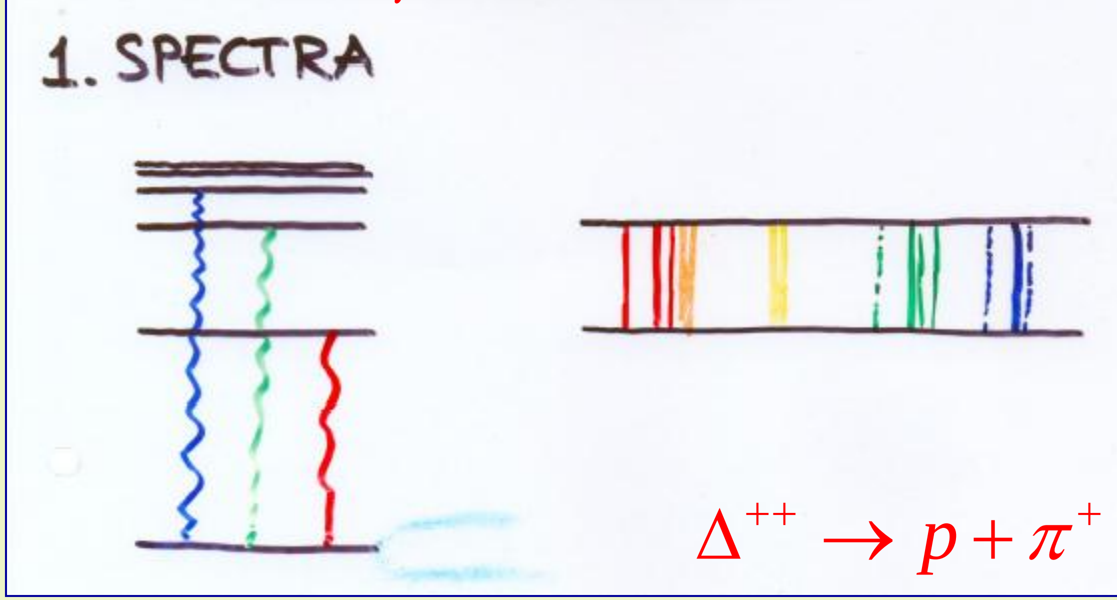

$$\Delta^{++} \rightarrow p + \pi^+$$

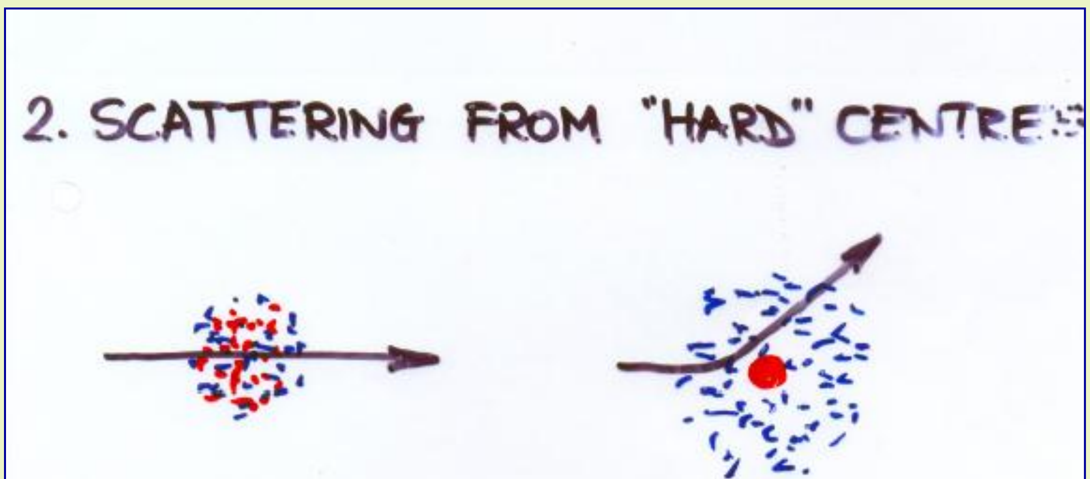

True from atoms to particles…..

Some observations are easier to interpret than others...

12

The Ace in Our Hands - cumulative processes.

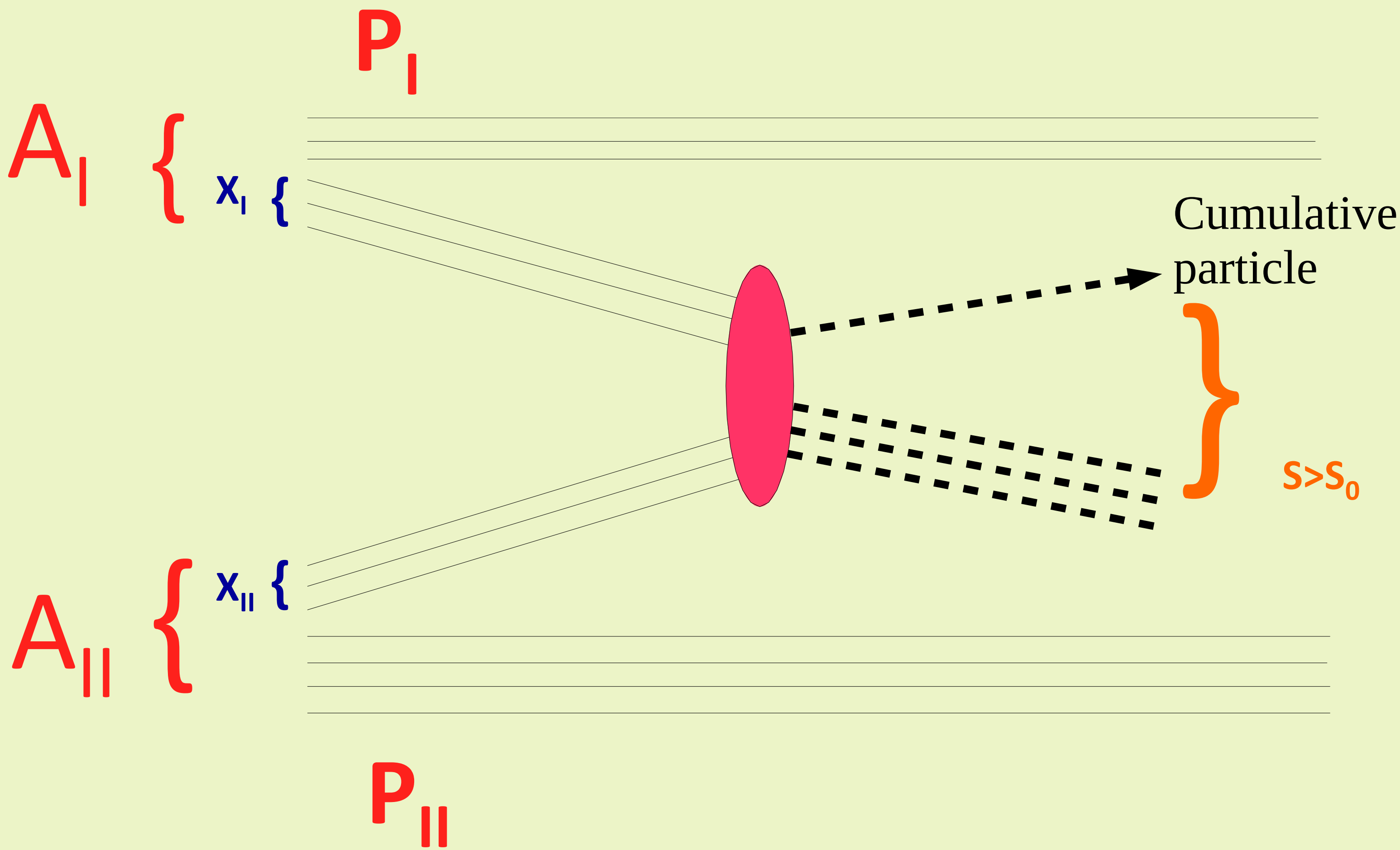

$$s_0 = \left(\frac{\mathbf{P}_{\mathbf{I}}}{\mathbf{A}_{\mathbf{I}}} + \frac{\mathbf{P}_{\mathbf{II}}}{\mathbf{A}_{\mathbf{II}}}\right)^2$$

- кинематическая граница для NN-взаимодействия

$$s_{cumulative} = (X_I \cdot \frac{P_I}{A_I} + X_{II} \cdot \frac{P_{II}}{A_{II}})^2$$

Кумулятивные и подпороговые процессы

$S_{cumulative} >> S_0$

$X_I \in [0, A_I]$ and $X_{II} \in [0, A_{II}]$

$X_I = X_{II} = 1$ - for free NN-interaction

kinematical borders

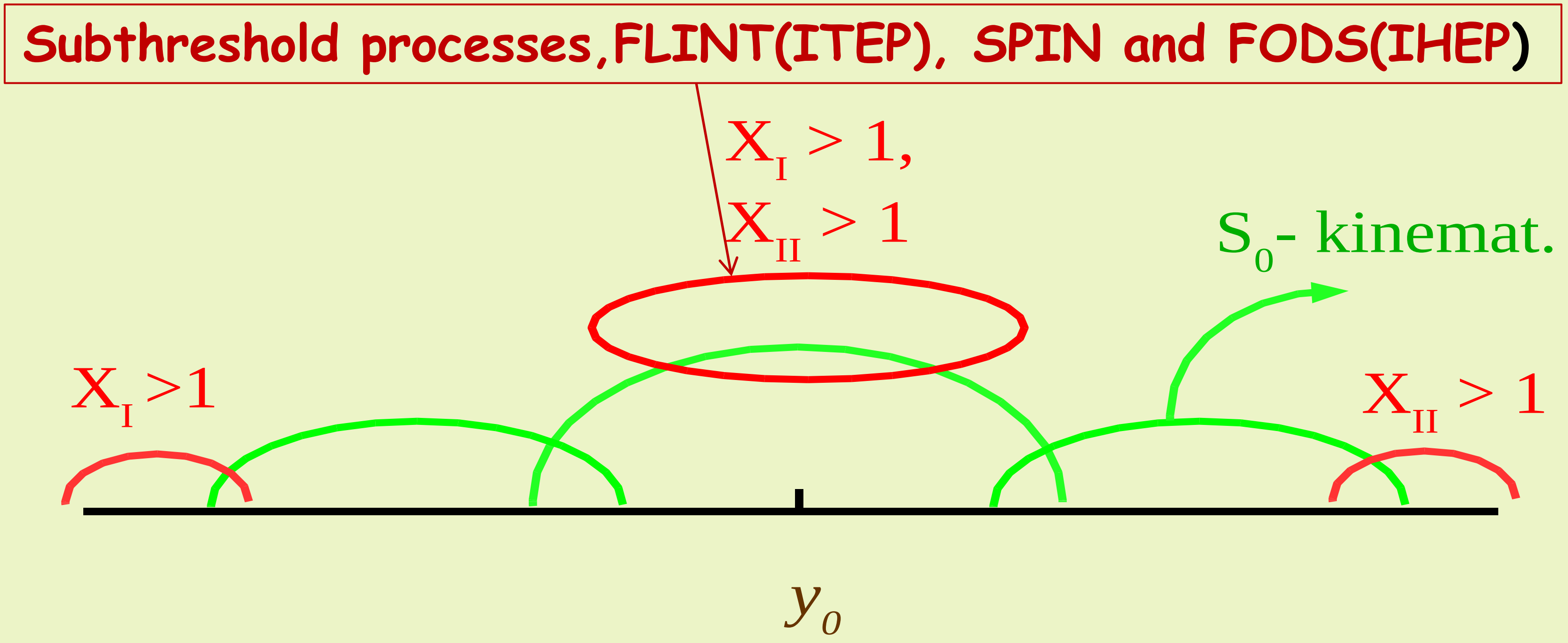

Cumulative processes:

1) $X_I = 1$ and $X_{II} > 1$ } Fragmentation
2) $X_{II} = 1$ and $X_I > 1$ } regions
3) $X_I > 1$ and $X_{II} > 1$ Central region

Stavinsky variables

V.S. Stavinski (1970's)

$\mu + N_{min} \cdot m \rightarrow m_c + [\, N_{min} \cdot m + \Delta]$

for $E_\mu >> m_i, E_c$

$$X = N_{\min} = Q \cong \frac{(E_c - \beta_\mu \cdot P_c \cdot \cos\theta_c)}{m} + \ldots \equiv X_I (X_{II})$$

AA-processes

V.S. Stavinsky JINR Rapid Communications N18-86, p.5 (1986)

$(X_I \cdot M_I) + (X_{II} \cdot M_{II}) \rightarrow m_c + [X_I \cdot M_I + X_{II} \cdot M_{II} + m_2]$

$$S_{\min}^{1/2} = \min(S^{1/2}) = \min[(X_I \cdot P_I + X_{\mathrm{II}} \cdot P_{II})^{1/2}]$$

A - dependence (1974-…)

$$\varepsilon\frac{d\sigma}{dp}(p+A\rightarrow\pi)\sim\begin{cases}A-\text{для\_тяжелых\_ядер}\\ A^{n>1}-\text{для\_лёгких\_ядер}\end{cases}$$

$$\varepsilon\frac{d\sigma}{dp}(p+A\rightarrow A')\sim\begin{cases}A^{5/3}-\text{для\_}d\\ A^{2}-\text{для\_}t\end{cases}$$

PHYSICAL REVIEW D VOLUME 11, NUMBER 11 1 JUNE 1975

Production of hadrons at large transverse momentum at 200, 300, and 400 GeV *

J. W. Cronin, H. J. Frisch, and M. J. Shochet
The Enrico Fermi Institute, University of Chicago, Chicago, Illinois 60637

J. P. Boymond, P. A. Piroué, and R. L. Sumner
Department of Physics, Joseph Henry Laboratories, Princeton University, Princeton, New Jersey 08540
(Received 5 December 1974)

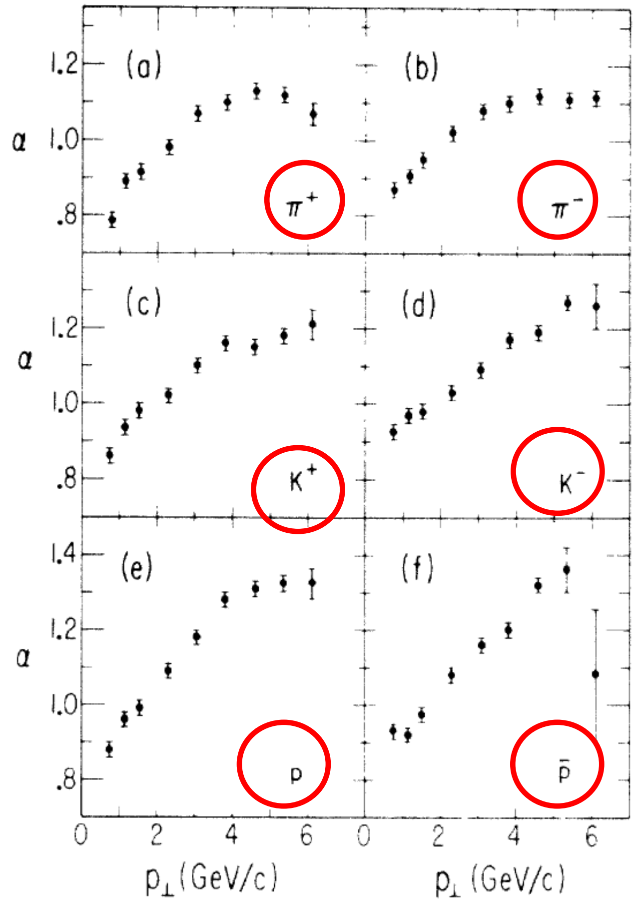

FIG. 17. Plots of the power α of the A dependence versus $p_\perp$ for the production of hadrons by 300-GeV protons; (a) π^+, (b) π^-, (c) K^+, (d) K^-, (e) p, and (f) $\bar{p}$.

A.A. Baldin's parameterization

Phys. At. Nucl. 56(3), p.385(1993)

$$\Pi = \frac{1}{2}(X_I^2 + X_{II}^2 + 2 \cdot X_I \cdot X_{II} \cdot \gamma_{I,II})^{\frac{1}{2}} = \frac{1}{2 \cdot m} \cdot S_{\min}^{\frac{1}{2}}$$

$$\gamma_{I,II} = \frac{(P_I \cdot P_{II})}{M_I \cdot M_{II}}$$

Inclusive data parameterization

$$E \cdot \frac{d^3\sigma}{dp^3} = C_1 \cdot A_I^{\frac{1}{3}+\frac{X_I}{3}} \cdot A_{II}^{\frac{1}{3}+\frac{X_{II}}{3}} \cdot \exp(-\frac{\Pi}{C_2}),$$

$$C_1 = 2200[mb \cdot GeV^{-2} \cdot c^3 \cdot sr^{-1}], C_2 = 0.127$$

C_1 and C_2 are constants

Cumulative processes.

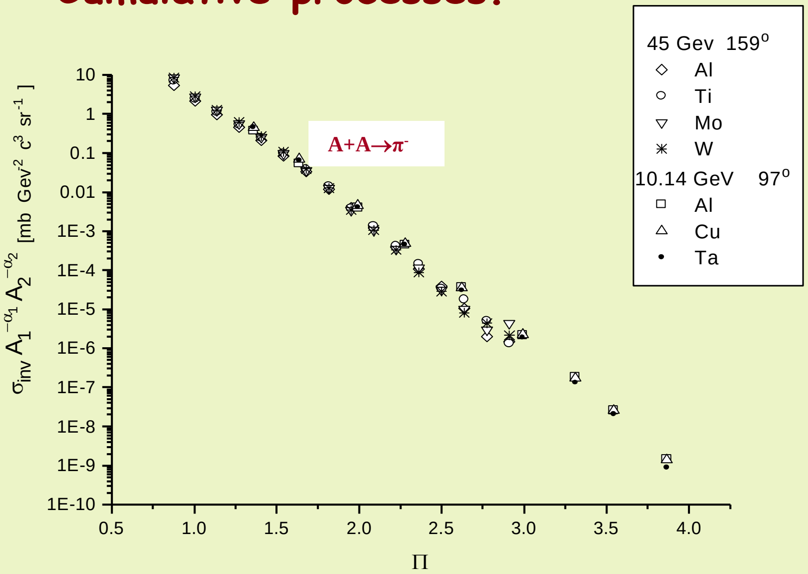

Twice cumulative processes.

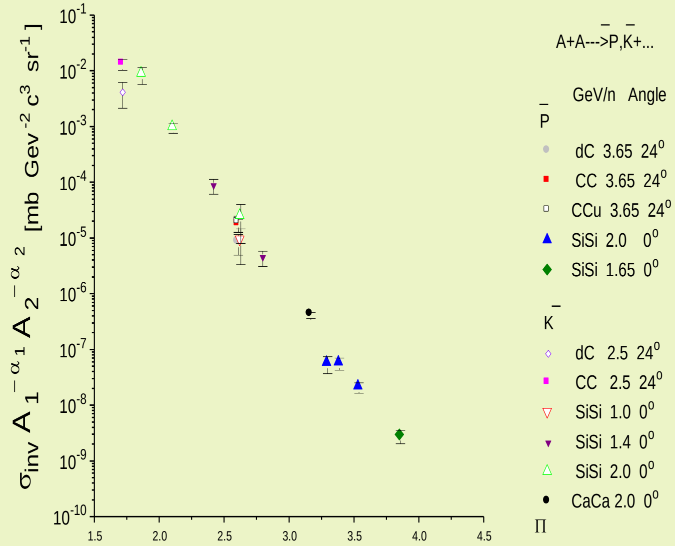

Twice cumulative deep subthreshold processes with heavy nuclei.

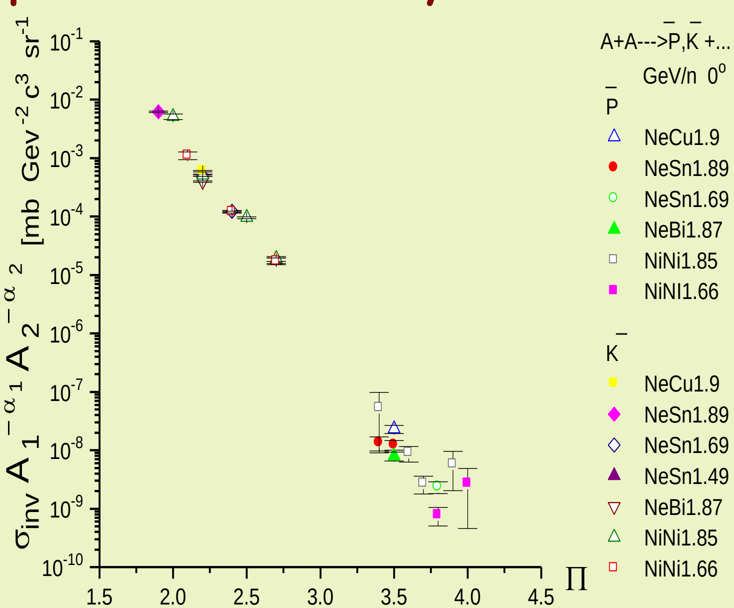

Antimatter production.

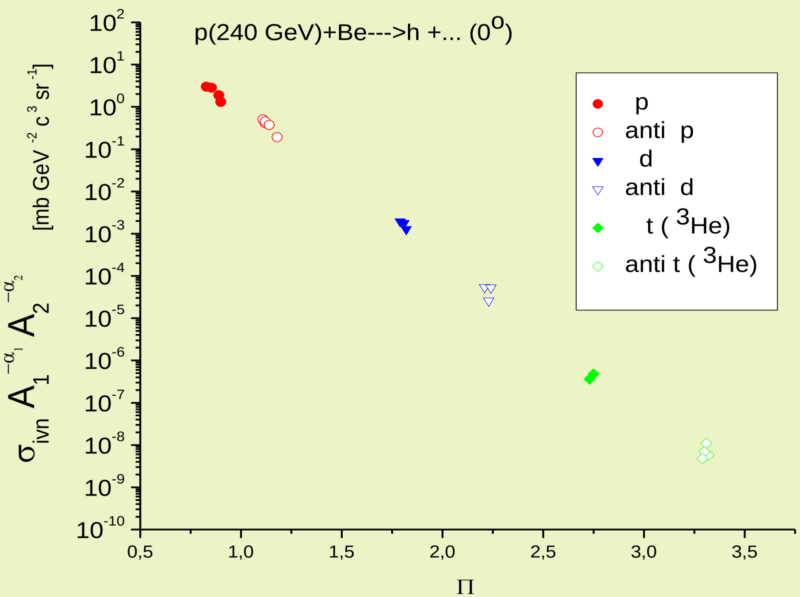

Fermi Motion and Short Range Correlation (SRC)

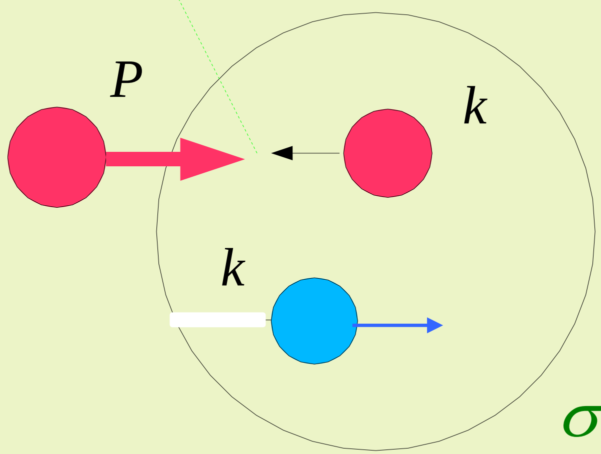

$$p + A \rightarrow \pi, \kappa, \bar{p}, \ldots + X$$

$$\sigma_\pi \sim n(\vec{k}) \cdot \sigma(NN \rightarrow \pi, K + X)$$

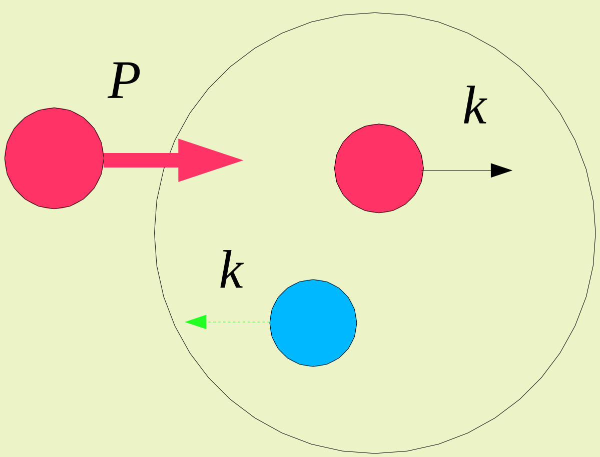

$$p + A \rightarrow n, p, \ldots + X$$

$$\sigma_N \sim n(\vec{k}) \cdot \sigma_0$$

Fluctons

$$p + A \rightarrow \pi, \kappa, \overline{p}, p, n, \ldots + X$$

$$\sigma_h \sim P_K \cdot G_{h/K}(K)$$

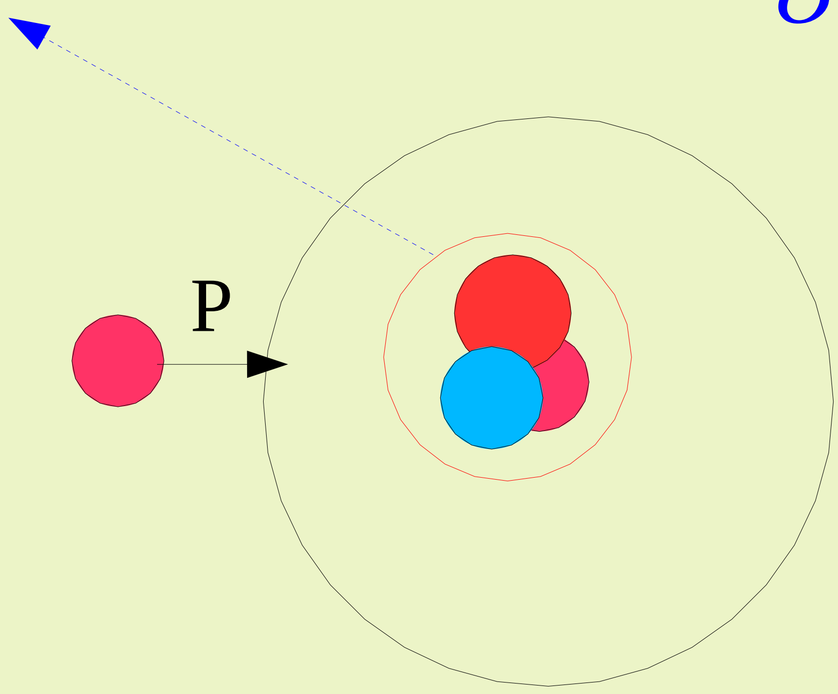

Seeing what the nucleons are made of

The deep inelastic scattering experiments made at SLAC in the 1960s established the quark-parton model and our modern view of particle physics

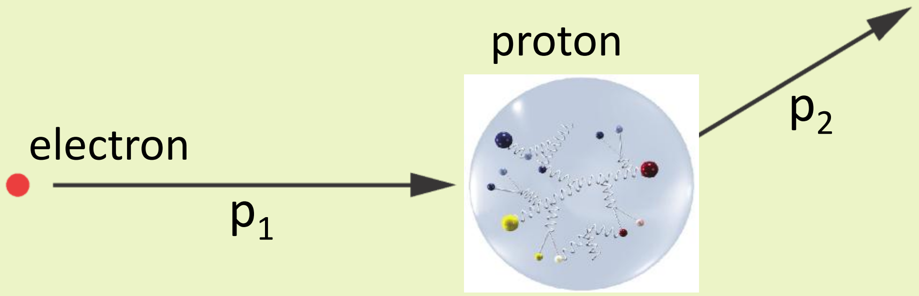

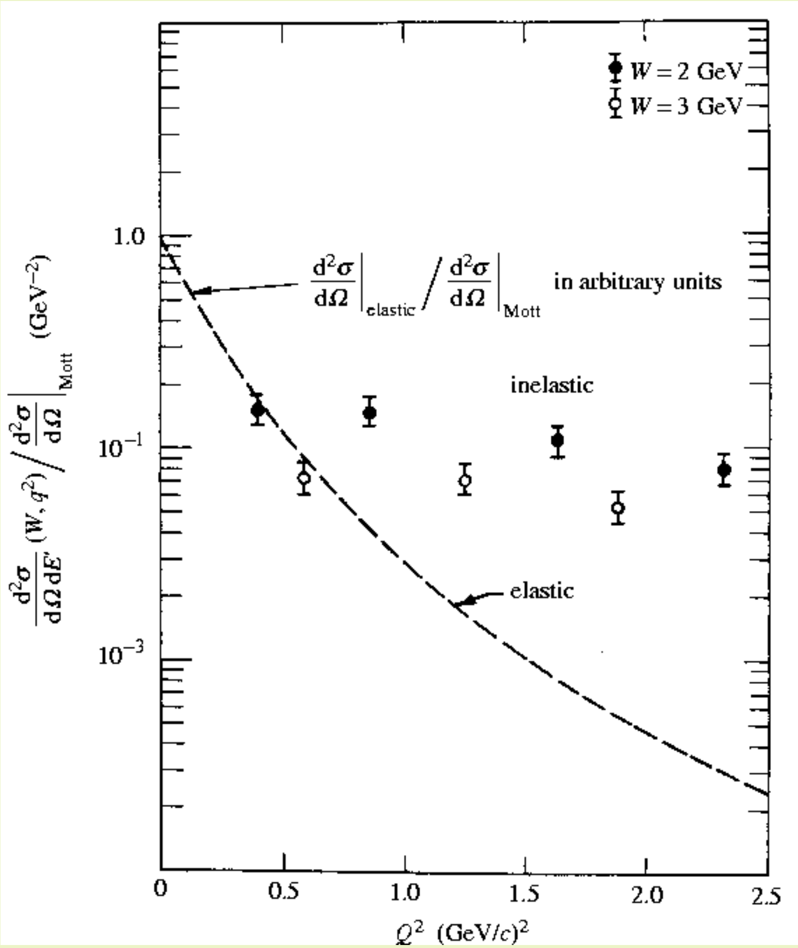

The angular distribution of the scattered electrons reflects the distribution of charge inside the proton

$\Rightarrow$ protons have point-like constituents
$\Rightarrow$ quarks

K.Rith From Nuclei to Nucleons (Summary)

Nuclear Physics A532 (1991) 3c-14c

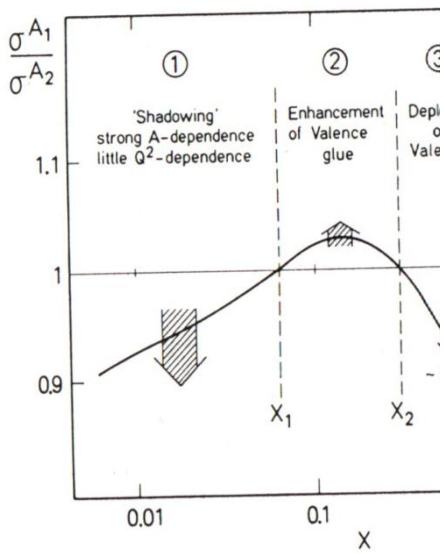

Figure 1. Global behaviour of nuclear effects

Region 1: $0 < x < x_1 \simeq 0.06$ $(z > 3\ \text{fm})$

In this region the dominant contributi quarks, the essential longitudinal distance action are $z > 3$ fm, much bigger than the si

than one. The effect (historically called 'Shadowing') increases with decreasing x, it increases strongly with atomic mass A and depends very little on Q^2. This behaviour is also observed in the antiquark distributions $\bar{q}(x)$, measured in the Drell-Yan process.

Region 2: $x_1 < x < x_2 \simeq 0.3$ $(3\ \text{fm} > z > 0.7\ \text{fm})$

$R^A(x)$ shows a small increase of a few percent above one. This enhancement varies very little with A and Q^2, it is definitively not due to seaquarks alone but probably dominantly a valence quark effect. There are indications that also the gluon distribution g(x) is enhanced in this region.

Region 3: $x_2 < x < x_3 \simeq 0.8$ $(z < 0.7\ \text{fm})$

In this region the sea quark distribution is essentially negligible and $R^A(x)$ reflects the behaviour of the valence-quark distributions. $R^A(x)$ is smaller than one with a minimum at $x \simeq 0.65$. The effect increases approximately like logA or the mean nuclear density $\bar{\rho}_A$.

Region 4: $x = 1$

This is the special region of quasielastic scattering where possibly effects of 'colour-transparency' could be observed.

Region 5: $x_3 < x < x_A$

For a nucleus with atomic mass A the quark distributions can in principle extend to $x_A = A$. $R^A(x)$ is bigger than one. Its behaviour is strongly influenced by Fermi-motion, final state interactions, nucleon-nucleon correlations, or the formation of multiquark clusters. Experimentally this region is essentially unexplored.

PHYSICAL REVIEW C VOLUME 45, NUMBER 4 APRIL 1992

Nuclear structure functions at $x > 1$

B. W. Filippone, R. D. McKeown, R. G. Milner,* and D. H. Potterveld†
Kellogg Radiation Laboratory, California Institute of Technology, Pasadena, California 91125

D. B. Day, J. S. McCarthy, Z. Meziani,‡ R. Minehardt, R. Sealock, and S. T. Thornton
Institute of Nuclear and Particle Physics and Department of Physics, University of Virginia, Charlottesville, Virginia 22901

J. Jourdan and I. Sick
Institut für Physik, Universität Basel, CH-4056, Basel, Switzerland

Z. Szalata
American University, Washington, D.C. 20016
(Received 19 April 1991)

Nuclear structure functions are extracted for high-energy electron scattering from nuclei at large values of the kinematic variable x and Q^2 in the range 1–4 $(\mathrm{GeV}/c)^2$. At the highest Q^2, the data for $x > 1$ begin to display a scaling indicative of local duality.

PACS number(s): 25.30.Fj, 13.60.Hb

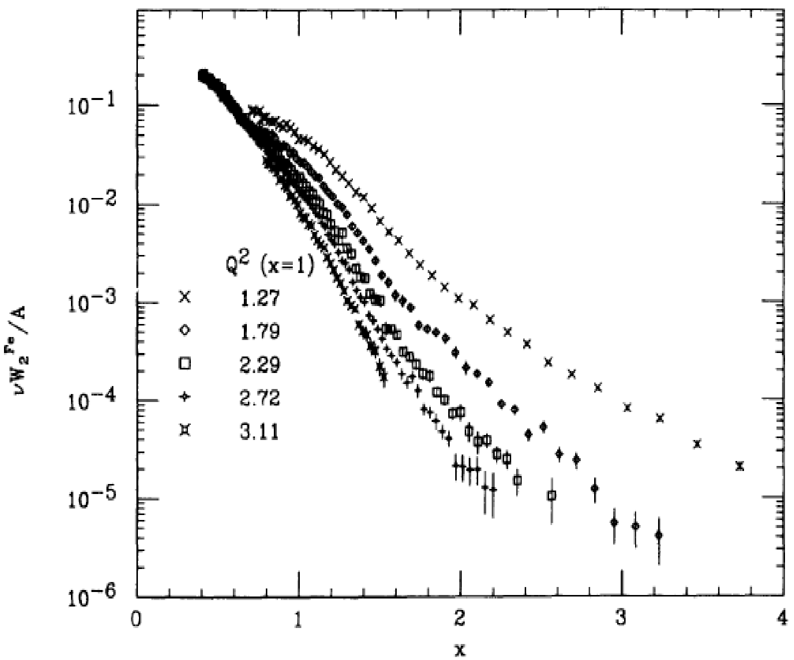

FIG. 1. Measured structure function per nucleon for Fe vs x. The Q^2 value at $x=1$ is also listed for the different kinematics.

INSTITUTE OF PHYSICS PUBLISHING JOURNAL OF PHYSICS G: NUCLEAR AND PARTICLE PHYSICS

J. Phys. G: Nucl. Part. Phys. **29** (2003) R1–R45 PII: S0954-3899(03)54926-X

TOPICAL REVIEW

Hadrons in the nuclear medium

M M Sargsian[1], J Arrington[2], W Bertozzi[3], W Boeglin[1], C E Carlson[4], D B Day[5], L L Frankfurt[6], K Egiyan[7], R Ent[8], S Gilad[3], K Griffioen[4], D W Higinbotham[8], S Kuhn[9], W Melnitchouk[8], G A Miller[10], E Piasetzky[6], S Stepanyan[8,9], M I Strikman[11] and L B Weinstein[9]

It is interesting to note that there is a clear gap between the kinematic regions of these two classes of experiments. This corresponds exactly to the optimal range for the study of the nucleonic degrees of freedom in nuclei, $1.5 \leqslant Q^2 \leqslant 4$ GeV^2, for which short-range correlations (SRCs) between nucleons can be resolved, and the quark degrees of freedom are only a small correction. Work at Jefferson Lab has started to fill this gap in a series of quasi-elastic $A(e, e')$, $A(e, e'N)$ and $A(e, e'N_1N_2)$ experiments. Previously, this range was just touched by inclusive experiments at SLAC [2–5] which also provided the first measurement of $A = 2, 3, 4$ form factors at large Q^2. A number of these high-energy experiments probe the light-cone projection of the nuclear wavefunction and in particular the light-cone nuclear density matrix, $\rho_A^N(\alpha, p_\perp)$, in the kinematics where the light-cone momentum fraction $\alpha \geqslant 1$ $(A \geqslant \alpha \geqslant 0)$ so that short-range correlations between nucleons play an important role.

eA-DIS

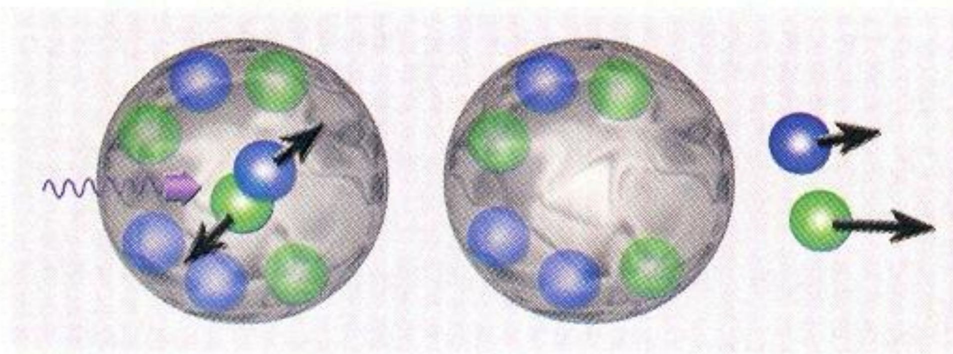

Fig. 1. Scattering of a virtual photon off a two-nucleon correlation, $x > 1.5$, before (left) and after (right) absorption of the photon.

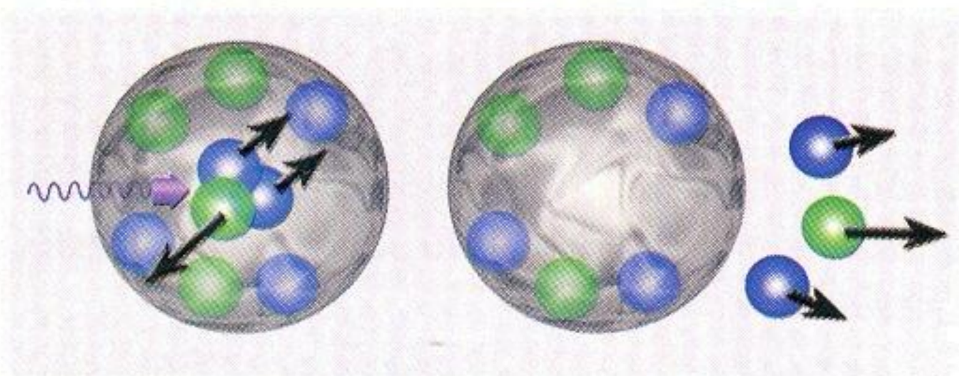

Fig. 2. Scattering of a virtual photon off a three-nucleon correlation, $x > 2$, before (left) and after (right) absorption of the photon.

eA scattering JLAB data

A.Stavinskiy, ITEP seminar, 11.4.2007

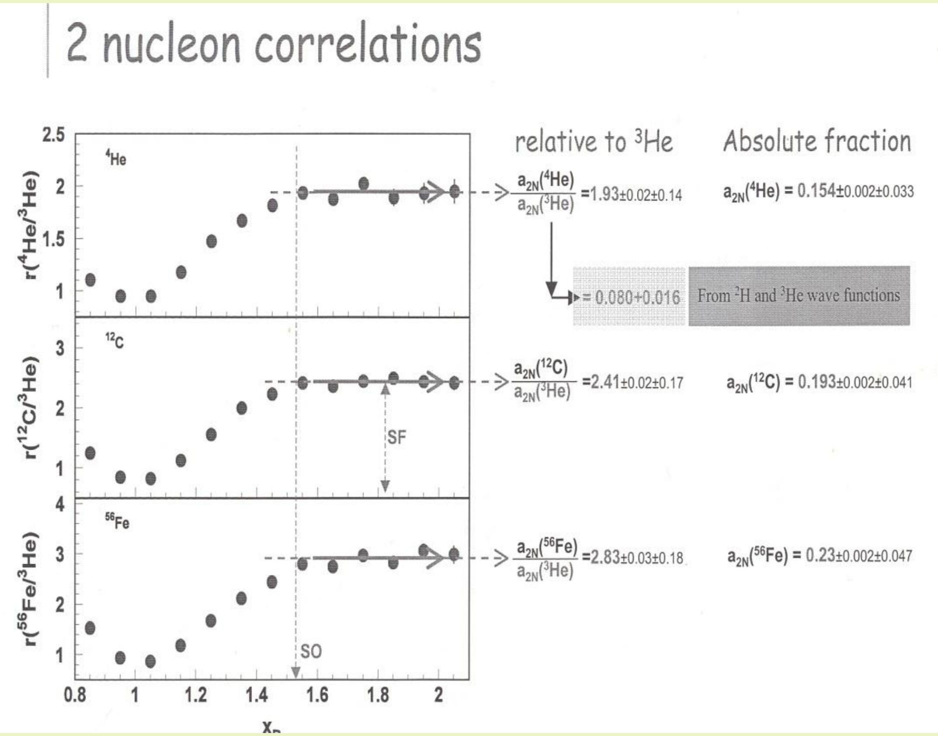

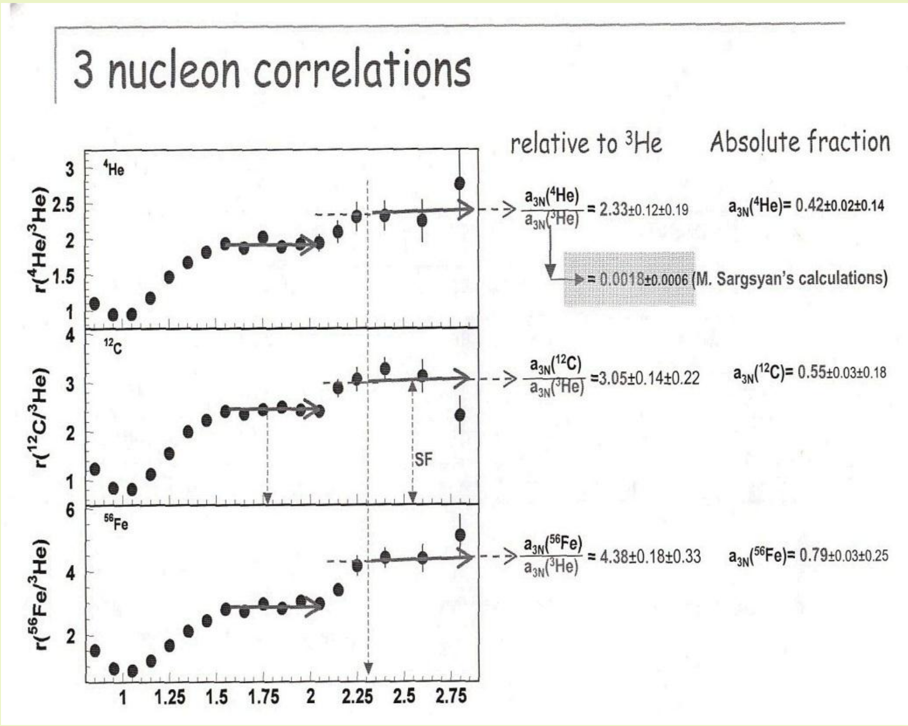

Having these data, we know almost full (≈99%) nucleonic picture of nuclei with $A \leq 56$

Fractions / Nucleus	Single particle (%)	2N SRC (%)	3N SRC (%)
^{56}Fe	**76** ± 0.2 ± 4.7	**23.0** ± 0.2 ± 4.7	**0.79** ± 0.03 ± 0.25
^{12}C	**80** ± 02 ± 4.1	**19.3** ± 0.2 ± 4.1	**0.55** ± 0.03 ± 0.18
^{4}He	**86** ± 0.2 ± 3.3	**15.4** ± 0.2 ± 3.3	**0.42** ± 0.02 ± 0.14
^{3}He	**92** ± 1.6	**8.0** ± 1.6	**0.18** ± 0.06
^{2}H	**96** ± 0.8	**4.0** ± 0.8	-----

Using the published data on (p,2p+n) [PRL,90 (2003) 042301] estimate the isotopic composition of 2N SRC in ^{12}C

$a_{pp}(^{12}C) \approx$ **4** ± **2** %

$a_{2N}(^{12}C) \approx$ **20** ± 0.2 ± 4.1 % → $a_{pn}(^{12}C) \approx$ **12** ± 4 %

$a_{nn}(^{12}C) \approx$ **4** ± **2** %

Volume 67B, number 1 PHYSICS LETTERS 14 March 1977

ТЕОРИЯ

LARGE MOMENTUM PION PRODUCTION IN PROTON NUCLEUS COLLISIONS AND THE IDEA OF "FLUCTUONS" IN NUCLEI

V.V. BUROV
The Moscow State University, Moscow, USSR

and

V.K. LUKYANOV and A.I. TITOV
Joint Institute for Nuclear Research, Dubna, USSR

Received 27 January 1977

It is shown that in proton-nucleus collisions, the production of pions with large momenta can be explained by the assumption of the existence of nuclear density fluctuations ("fluctuons") at short distances of the nucleon core radius order, with the mass of several nucleons.

The purpose of this note is to realize the idea [4] that the cumulative effect is connected largely with a suggestion on the existence in nuclei of the so-called fluctuons. Earlier fluctuons were proposed [7] in order to understand the nature of the "deuteron peak" in the pA-scattering cross section at large momentum transfers [8] and also to interpret the pd-scattering

cross section [9]. Compressional fluctuations of mass $M_k = km_p$ of nucleons in the small volume $V_\xi = \frac{4}{3}\pi r_\xi^3$ where r_ξ is the fluctuon radius were assumed.

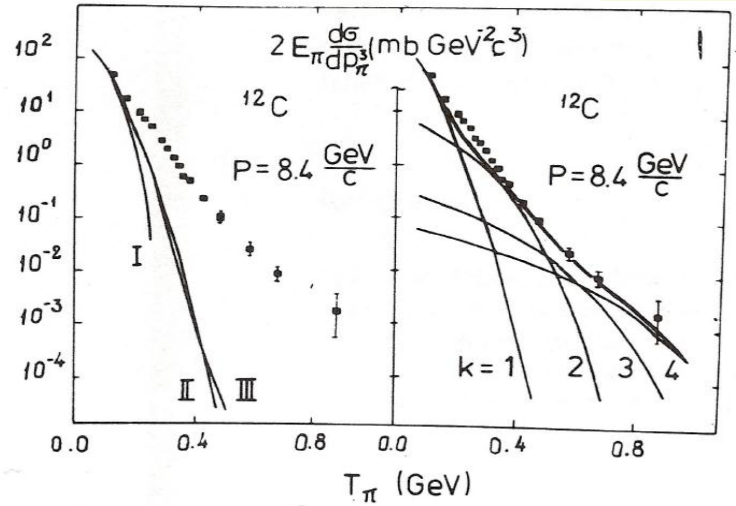

Fig. 1. (a) Calculations of the invariant pion production cross section for ^{12}C: I – for the free proton target; II – with fermi motion; III – the relativization effect. (b) The contributions of separate fluctuons with mass $M_k = km_p$ where k is the order of cumulativity.

Fluctons Probability inside nuclei

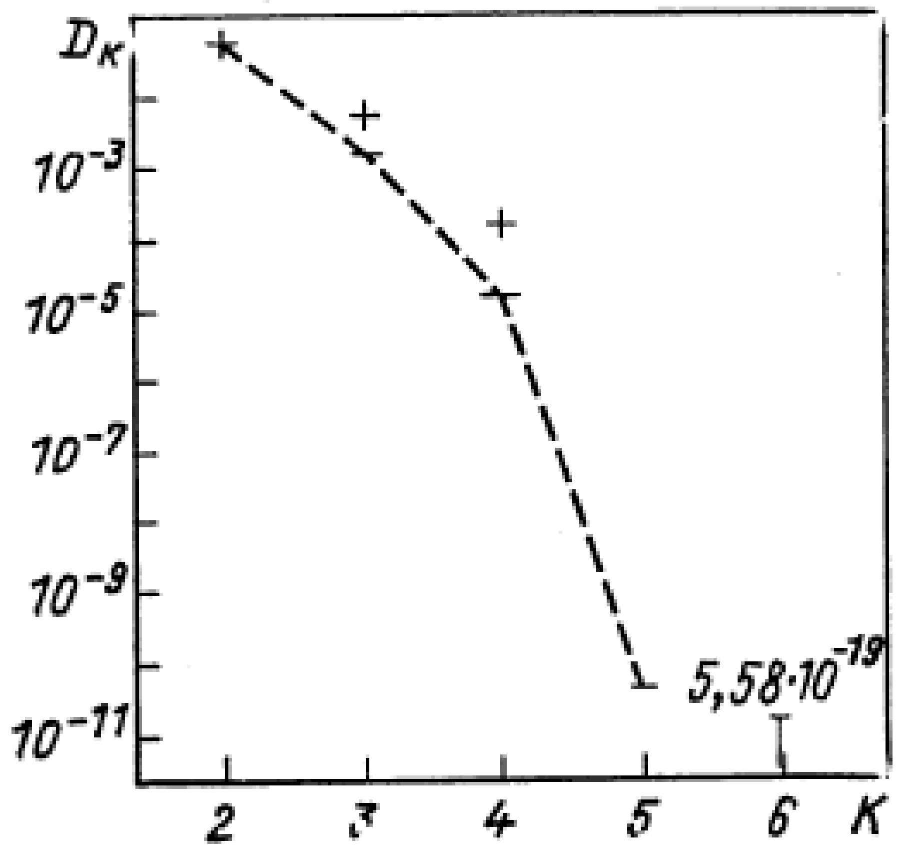

Рис. 19. Вероятность существования флуктонов с k нуклонами в ядрах

^{12}C - structure

RNP - program at JINR

V.V.B., V.K.Lukyanov, A.I.Titov, PLB, 67, 46(1977)

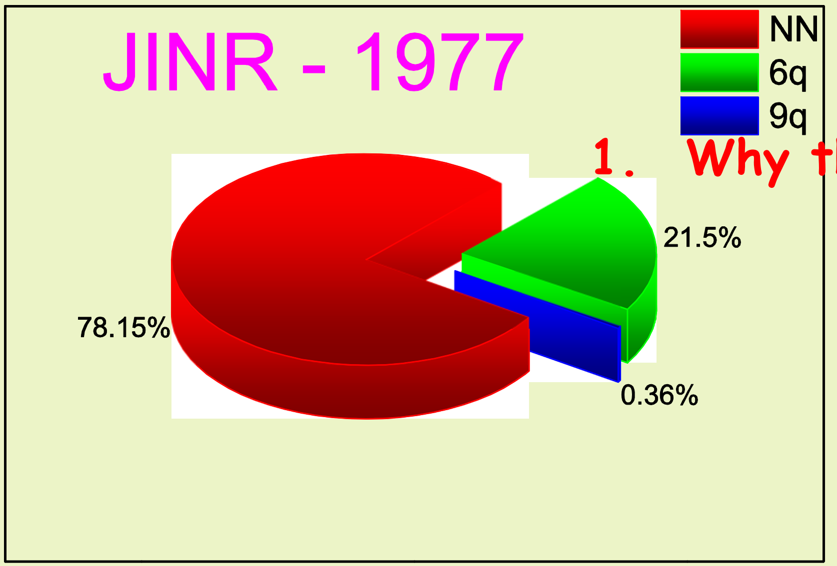

eA - program at JLab

R.Subedi et al., Science 320 (2008) 1476-1478
e-Print: arXiv:0908.1514 [nucl-ex]

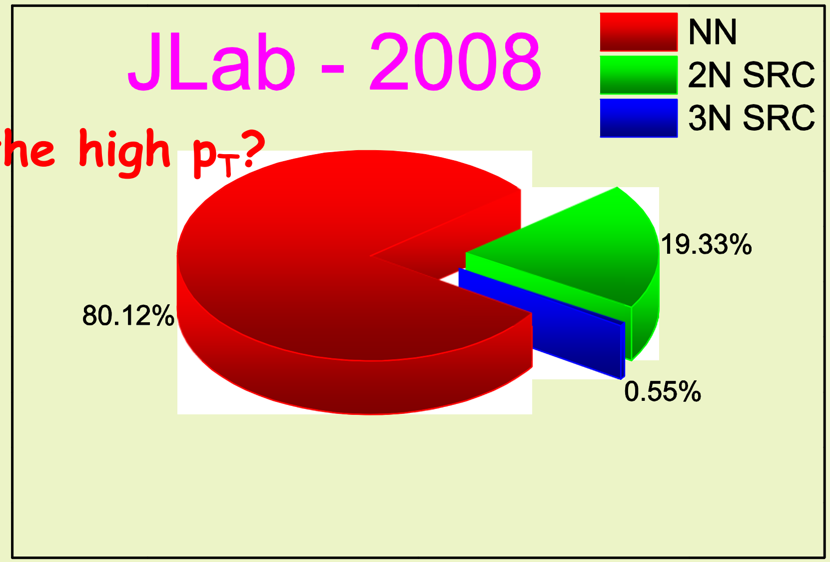

1. Why the high p_T?

Probing of compact baryonic configurations in nuclei in $A(p, \bar{p})X$ reactions and antiproton formation length in nuclear matter

Yu. T. Kiselev,[1,*] V. A. Sheinkman,[1] A. V. Akindinov,[1] M. M. Chumakov,[1] A. N. Martemyanov,[1] V. A. Smirnitsky,[1] Yu. V. Terekhov,[1] and E. Ya. Paryev[2]

[1]*Institute for Theoretical and Experimental Physics, Moscow 117218, Russia*

[2]*Institute for Nuclear Research, Russian Academy of Sciences, Moscow 117312, Russia*

(Dated: May 15, 2012)

Inclusive cross sections $\sigma^A = Ed^3\sigma(X, P_t^2)/d^3p$ of antiproton and negative pion production on Be, Al, Cu and Ta targets hit by 10 GeV protons were measured at the laboratory angles of 10.5° and 59°. Antiproton cross sections were obtained in both kinematically allowed and kinematically forbidden regions for antiproton production on a free nucleon. The antiproton cross section ratio as a function of the longitudinal variable X exhibits three separate plateaus which gives evidence for the existence of compact baryon configurations in nuclei—small-distance scaled objects of nuclear structure. Comparability of the measured cross section ratios with those obtained in the inclusive electron scattering off nuclei suggests a weak antiproton absorption in nuclei. Observed behavior of the cross section ratios is interpreted in the framework of a model considering the hadron production as a fragmentation of quarks (antiquarks) into hadrons. It has been established that the antiproton formation length in nuclear matter can reach the magnitude of 4.5 fm.

Phys.Rev. C85 (2012) 054904

Phys.Rev. C85 (2012) 054904

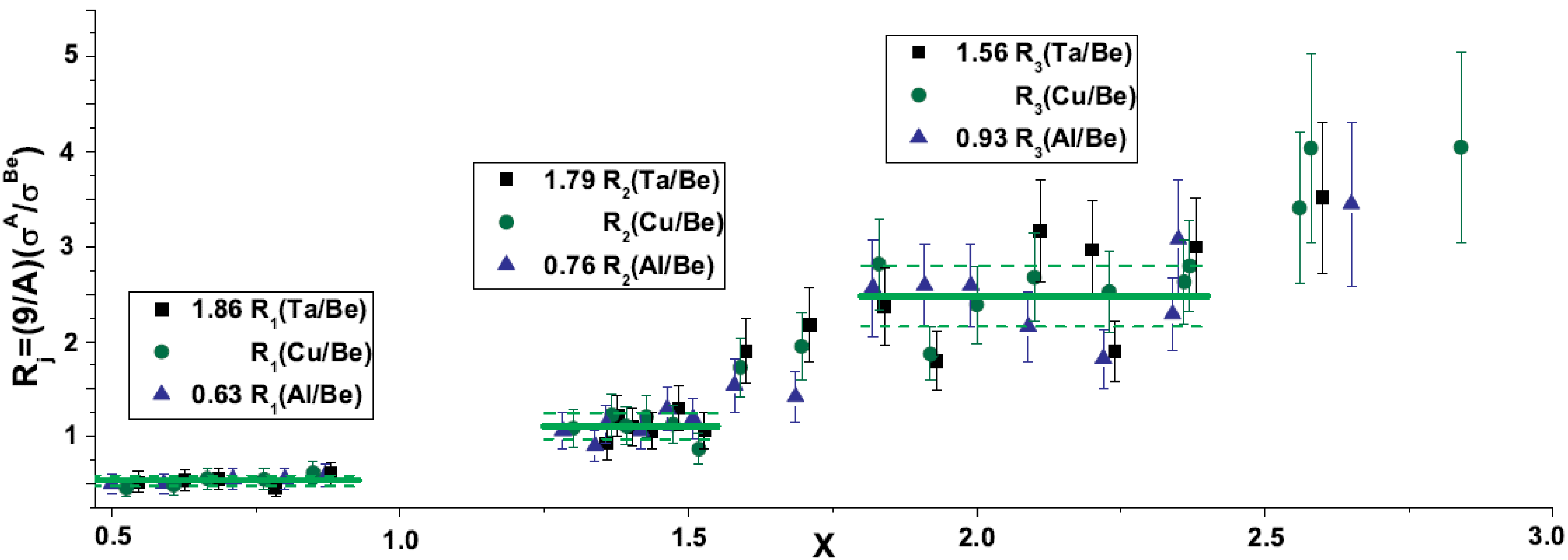

FIG. 1. (Color online) Cross section ratio $R = (9\sigma_{pA\to\bar{p}})/(A\sigma_{p\text{Be}\to\bar{p}})$ as a function of X in the range $0.5 < X < 2.8$. Values of the rescaling factors for $j = 1, 2, 3$ are indicated in the legends from left to right, respectively. Solid and dashed lines correspond to the weighted average magnitudes of $R(\text{Cu/Be})$ and their errors shown in Table V. Symbols for Al/Be and Ta/Be ratios are slightly displaced.

Why the high p_T?

The Counting rules

In 1973 were published two artiles :

Matveev V.A., Muradyan R.M., Tavkhelidze A.N. Lett. Nuovo Cimento 7,719 (1973);

Brodsky S., Farrar G. Phys. Rev. Lett. 31,1153 (1973)

Predictions that for momentum $p_{beam} \geq 5$ GeV/c in any binary large-angle scattering ($\theta_{cm} > 40°$) reaction at large momentum transfers $Q = \sqrt{-t}$:

$$A + B \to C + D$$

$$\frac{d\sigma}{dt}_{A+B\to C+D} \sim s^{-(n_A+n_B+n_C+n_D-2)} f\left(\frac{t}{s}\right)$$

where n_A, n_B, n_C and n_D the amounts of elementary constituents in A,B,C and D.

$s=(p_A+p_B)^2$ and $t=(p_A-p_C)^2$,

$$\frac{d\sigma}{dt}_{pp\to pp} \sim S^{-10} \quad \text{and} \quad \frac{d\sigma}{dt}_{\pi p\to \pi p} \sim S^{-8}$$

SLAC – PUB – 4749
October 1988
(M)

ANTIPROTON ANNIHILATION IN QUANTUM CHROMODYNAMICS*

STANLEY J. BRODSKY

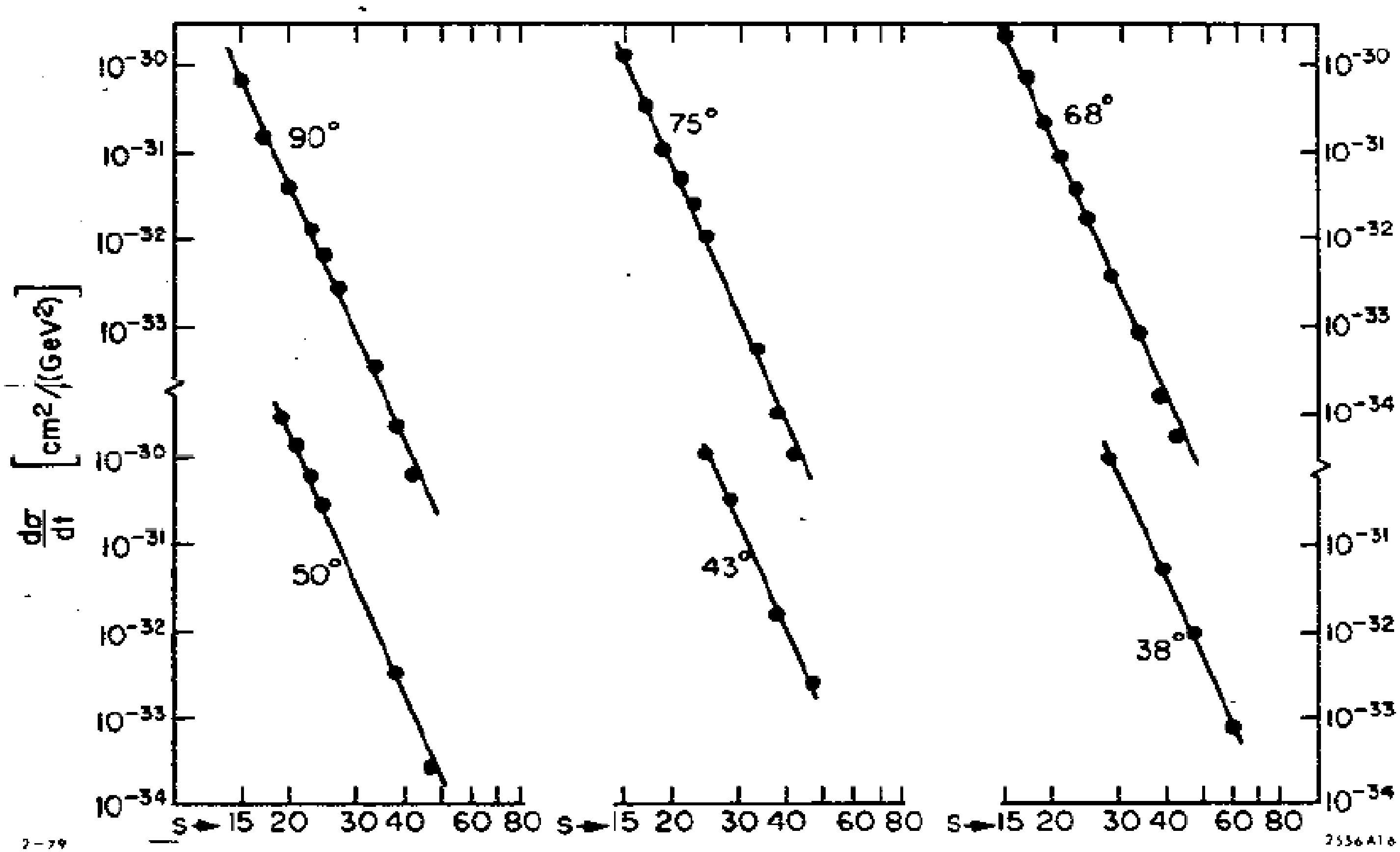

Fig. 16. Test of fixed θ_{CM} scaling for elastic pp scattering. The best fit gives the power $N = 9.7 \pm 0.5$ compared to the dimensional counting prediction $N=10$. Small deviations are not readily apparent on this log-log plot. The compilation is from Landshoff and Polkinghorne.

QCD Phenomenology

Lectures at the CERN–Dubna School, Pylos, August 2002

Yu.L. Dokshitzer
LPTHE, University Paris-6, France
and
PNPI, St. Petersburg, Russia

Abstract
The status of QCD phenomena and open problems are reviewed

CERN 2004-001

2.3 Where is confinement?

The quark–gluon picture works rather well across the board. Moreover, in many cases it seems to work *too well*. This is another worry: too good to be true ain't good enough.

Too early?

The way the differential large angle $2 \to 2$ particle scattering cross sections should scale with energy (momentum transfer) was envisaged by the so-called "quark counting rules" [26],

$$\frac{d\sigma}{dt} = \frac{f(\Theta)}{s^{K-2}}; \qquad \frac{t}{s} = \text{const},$$

with K the number of *elementary fields* (quarks, photons, leptons, etc.) among / inside the initial and final particles.

For example, in the case of the deuteron break-up by a photon, $\gamma + D \to p + n$, we have $K = 1 + 6 + 6 = 13$ (a photon and 6 quarks inside the initial deuteron and another 6 in the final proton and neutron). So, the differential cross section is expected to fall with s, *asymptotically*, as $s^{-11} = E_{\rm c.m.}^{-22}$. The key word *asymptotically* always provided an excuse for unnerved HEP theorists in their encounters with angered experimenters. The JLAB plot in Fig. 1 which I borrowed from Paul Hoyer's talk [27] seems to be telling us that this standard excuse is unnecessary here. However, it is again unnerving but for precisely opposite reason, if you take my meaning. Indeed, it is *very difficult* to digest how the naive asymptotic regime manage to settle *that* early! The lab. energy $1\,\text{GeV}$ of the incident photon, where the scaling behaviour starts, is just *too* low.

The "counting rules" invite us to view a fast deuteron as a system of six comoving valence quarks. One of them is punched by the photon. The other five we have to properly push ourselves so as to make them fit into two outgoing nucleons. This is done by exchanging five gluons between the quarks in the *scattering amplitude* so that the *cross section* acquires the factor α_s^{10}. The picture makes sense as long as 1) the deuteron is indeed *fast* and 2) typical momentum transfers q^2 between quarks are large enough to allow us to use the concept of gluon exchange and of the QCD$^{(1)}$ coupling $\alpha_s(q^2)$ for that matters. None of these conditions holds for $E_\gamma \simeq 1\,\text{GeV}$.

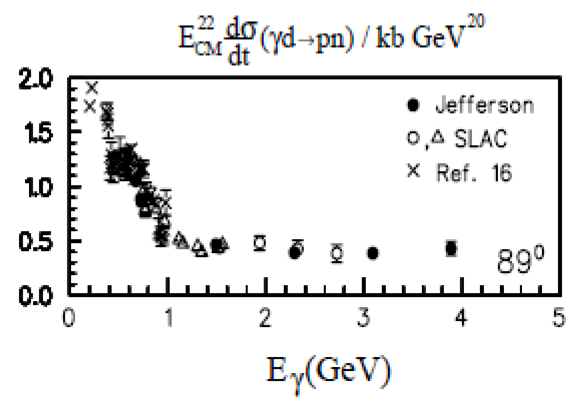

Fig. 1: Large angle γ-disintegration of a deuteron [28].

Nonetheless we would have had every right to feel happy about Fig. 1 provided we could convincingly answer but one question: why is such precocious scaling not seen for simpler systems and in particular for the simplest of them all – the electromagnetic form factor of a pion?

Light-Front QCD*

Stanley J. Brodsky

SLAC–PUB–10871
November 2004

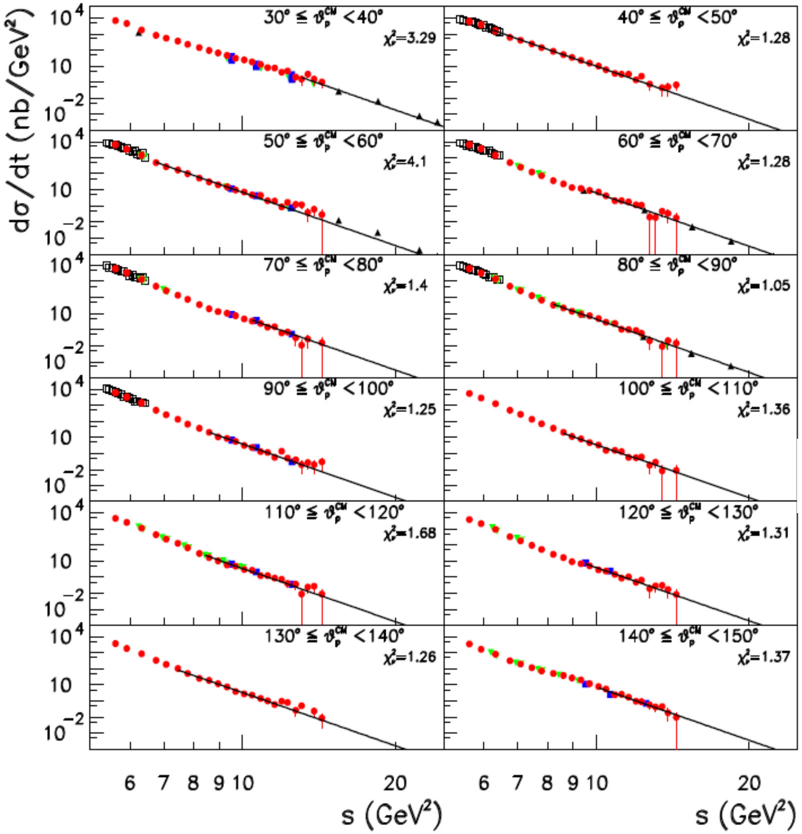

$s^{11}\frac{d\sigma}{dt}(\gamma d \to pn) \sim$ constant at fixed CM angle

Figure 8: Fits of the cross sections $d\sigma/dt$ to s^{-11} for $P_T \geq P_T^{th}$ and proton angles between 30° and 150° (solid lines). Data are from CLAS (full/red circles), Mainz(open/black squares), SLAC (full-down/green triangles), JLab Hall A (full/blue squares) and Hall C (full-up/black triangles). Also shown in each panel is the χ^2_ν value of the fit. From Ref. [160].

Pis'ma v ZhETF, vol. 81, iss. 7, pp. 387 – 390

Indication of asymptotic scaling in the reactions $dd \to p^3$H, $dd \to n^3$He and $pd \to pd$

Yu. N. Uzikov[1)]
Joint Institute for Nuclear Research, LNP, 141980 Dubna, Moscow region, Russia

Submitted 11 January 2005
Resubmitted 28 February 2005

It is shown that the differential cross sections of the reactions $dd \to n^3$He and $dd \to p^3$H measured at c.m.s. scattering angle $\theta_{cm} = 60^\circ$ in the interval of the deuteron beam energy 0.5–1.2 GeV demonstrate the scaling behaviour, $d\sigma/dt \sim s^{-22}$, which follows from constituent quark counting rules. It is found also that the differential cross section of the elastic $dp \to dp$ scattering at $\theta_{cm} = 125 - 135^\circ$ follows the scaling regime $\sim s^{-16}$ at beam energies 0.5–5 GeV. These data are parameterized here using the Reggeon exchange.

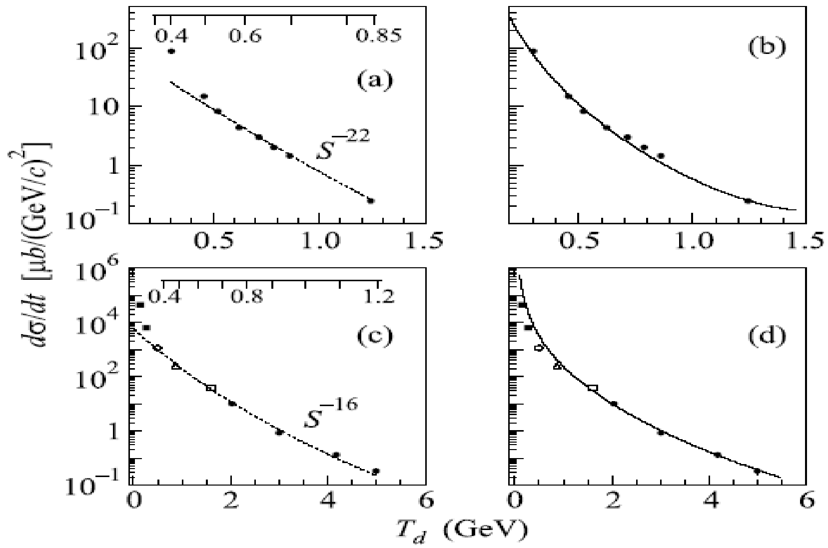

Fig.2. The differential cross section of the $dd \to n^3$He and $dd \to p^3$H reactions at $\theta_{cm} = 60^o$ (a), (b) and $dp \to dp$ at $\theta_{cm} = 127^o$ (c), (d) versus the deuteron beam kinetic energy. Experimental data in (a), (b) are taken from [20]. In (c), (d), the experimental data (black squares), (○), (△), (open square) and (●) are taken from [22 – 26], respectively. The dashed curves give the s^{-22} (a) and s^{-16} (c) behaviour. The full curves show the result of calculations using Regge formalism given by Eqs. (2), (3), (4) with the following parameters: (b) – $C_1 = 1.9\,\mathrm{GeV}^2$, $R_1^2 = 0.2\,\mathrm{GeV}^{-2}$, $C_2 = 3.5$, $R_2^2 = -0.1\,\mathrm{GeV}^{-2}$; (d) – $C_1 = 7.2\,\mathrm{GeV}^2$, $R_1^2 = 0.5\,\mathrm{GeV}^{-2}$, $C_2 = 1.8$, $R_2^2 = -0.1\,\mathrm{GeV}^{-2}$. The upper scales in (a) and (c) show the relative momentum q_{pn} (GeV/c) in the deuteron for the ONE mechanism

Which p_T and x_T are interesting?

pp -> pp (90^0)

C.W. Akerlof et al., Phys.Rev., vol.159, N5, 1138-1149, 1967

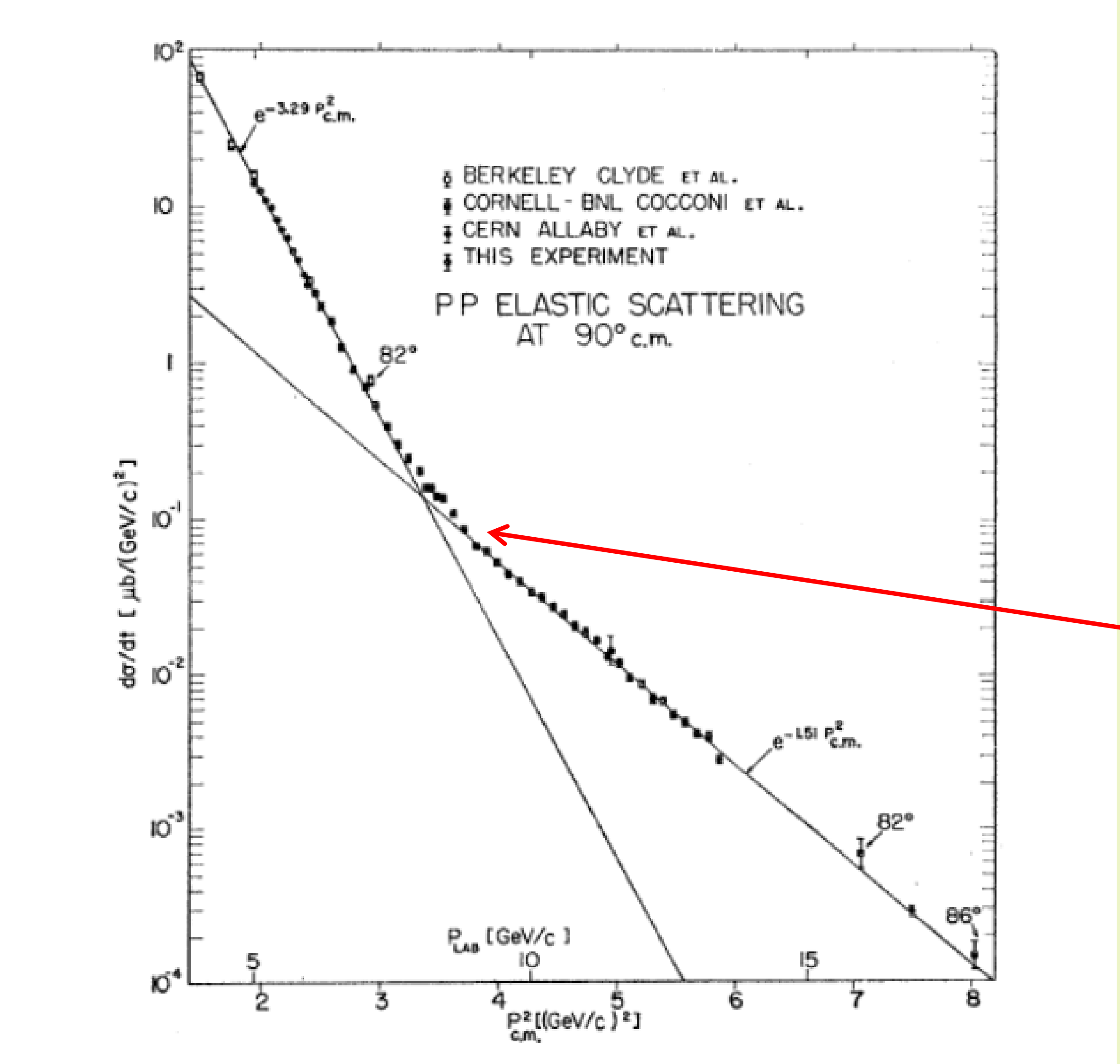

p_T ~ 2 GeV/c

$p\uparrow p\uparrow \rightarrow pp(90^0)$

E.A. Crosbie et al., Phys.Rev. D, vol.23, N3,1981

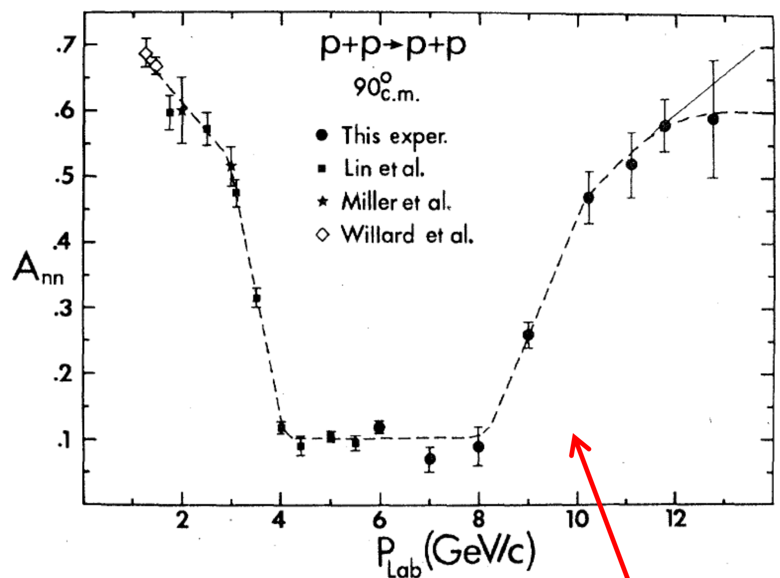

FIG. 2. Plot of the spin-spin correlation parameter A_{nn} for $p+p\rightarrow p+p$ at $90°_{c.m.}$ as a function of incident beam momentum. The dashed and solid lines are hand-drawn possible fits.

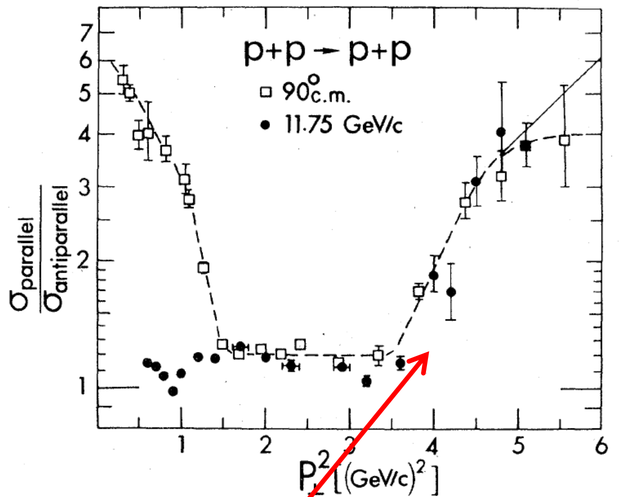

FIG. 3. Plot of the ratio of the spin-parallel to spin-antiparallel differential cross sections, as a function of $P_\perp^2$, for p-p elastic scattering. The squares are the fixed-angle data at $90°_{c.m.}$, with the incident energy varied. The circles are data (Refs. 5, 11) with the momentum held fixed at 11.75 GeV/c while the scattering angle is varied. The dashed and solid lines are hand-drawn possible fits to the $90°_{c.m.}$ data.

p_T ~ 2 GeV/c

$p\,\bar{p}$

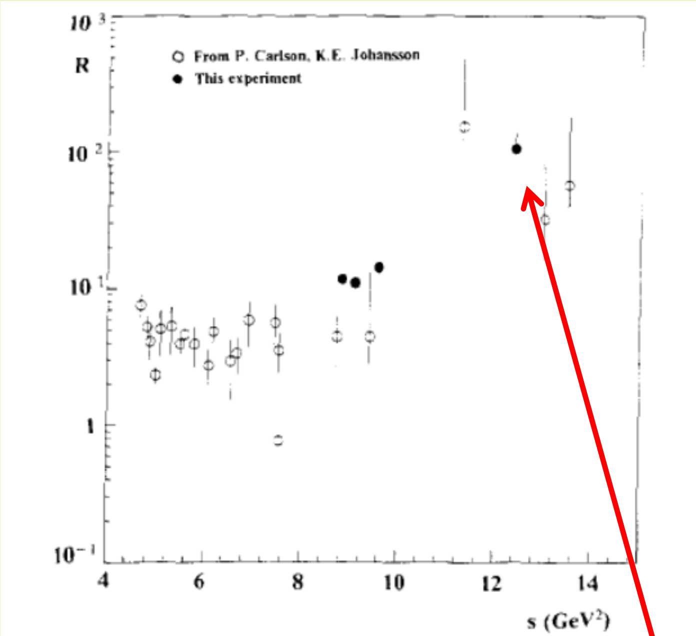

$$R = \frac{\sigma(pp \to pp)}{\sigma(\bar{p}p \to \bar{p}p)}(90^{o}\,c.m.)$$

p_T ~ 2 GeV/c region

Cross-sections at 90 degrees

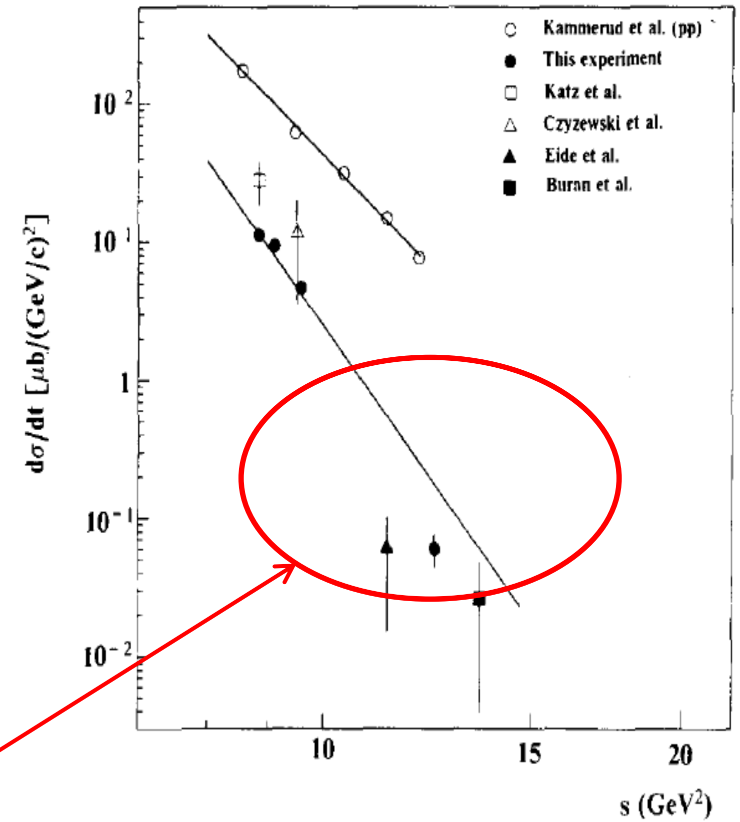

Fig. 3. The p$\bar{p}$ and pp elastic differential cross sections at 90° CM as function of the square of the CM energy, s. Open circles are pp data from ref. [6]. These data fit well to the drawn curve proportional to s^{-9}. The remaining points are p$\bar{p}$ data. Shaded from this experiment. Otherwise from ref. [7] (open square), ref. [8] (open triangle) ref. [9] (shaded triangle) and ref. [10] (shaded square). The lower curve is an s^{-n} fit to four data points of this experiment, neglecting systematic errors. One obtains $n = 12.3 \pm 0.2$, but evidently the data do not seem to follow this kind of a power law.

C. Baglin et al., Phys.Lett. B, vol.225, N3, 296-300, 1989

High p_T + NUCLEI

Color Transparency

arXiv:1208.3668v1 [nucl-th] 17 Aug 2012

Gerald A. Miller

Physics Department, Univ. of Washington, Seattle, Wa. 98195-1560, USA

Abstract. Color transparency is the vanishing of nuclear initial or final state interactions involving specific reactions. The reasons for believing that color transparency might be a natural consequence of QCD are reviewed. The main impetus for this talk is recent experimental progress, and this is reviewed briefly.

The basic idea is that some times a hadron is in a color-neutral point-like configuration PLC. If such undergoes a coherent reaction, in which one sums gluon emission amplitudes to calculate the scattering amplitude, the PLC does not interact with the surrounding media. A PLC is not absorbed by the nucleus. The nucleus casts no shadow. This is a kind of quantum mechanical invisibility.

SUMMARY

Color transparency is an expected, but not certain, consequence of QCD. It has been observed at high energies at FermiLab. Evidence at medium energy is piling up. It seems that PLC formation is an important part of (single) meson production at large values of Q^2, but has not yet been observed for the nucleon.

Color(nuclear) transparency in 90^0 c.m. quasielastic $A(p,2p)$ reactions

The incident momenta varied from 5.9 to 14.4 GeV/*c*, corresponding to $4.8 < Q^2 < 12.7$ $(\mathrm{GeV}/c)^2$.

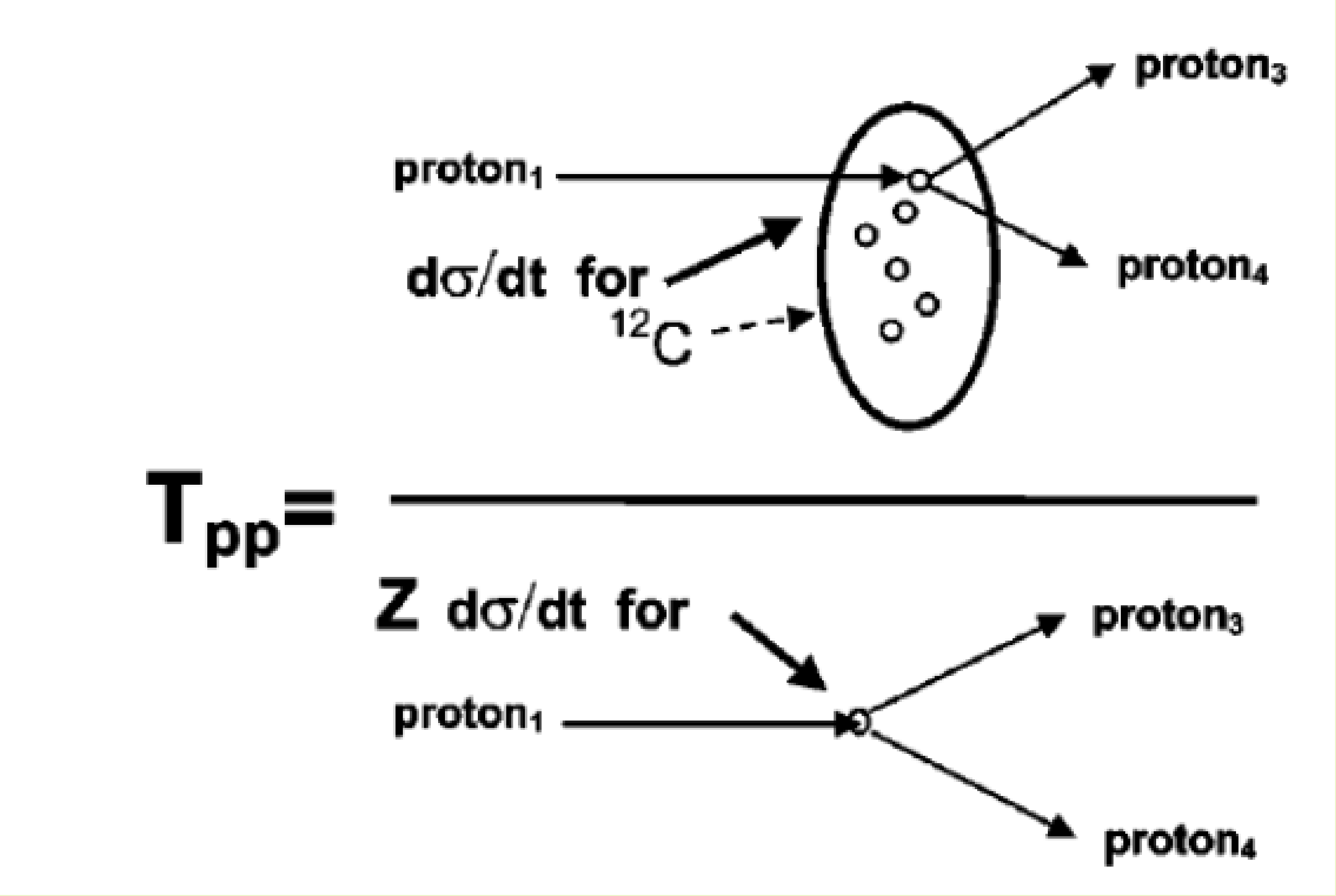

Color(nuclear) transparency

VOLUME 87, NUMBER 21 PHYSICAL REVIEW LETTERS 19 NOVEMBER 2001

Energy Dependence of Nuclear Transparency in C(p,2p) Scattering

A. Leksanov,[5] J. Alster,[1] G. Asryan,[3,2] Y. Averichev,[8] D. Barton,[3] V. Baturin,[5,4] N. Bukhtoyarova,[3,4] A. Carroll,[3] S. Heppelmann,[5] T. Kawabata,[6] Y. Makdisi,[3] A. Malki,[1] E. Minina,[5] I. Navon,[1] H. Nicholson,[7] A. Ogawa,[5] Yu. Panebratsev,[8] E. Piasetzky,[1] A. Schetkovsky,[5,4] S. Shimanskiy,[8] A. Tang,[9] J. W. Watson,[9] H. Yoshida,[6] and D. Zhalov[5]

$$T_{\rm CH} = T \int d\alpha \int d^2\vec{P}_{FT}\, n(\alpha, \vec{P}_{FT}) \frac{(\frac{d\sigma}{dt})_{pp}(s(\alpha))}{(\frac{d\sigma}{dt})_{pp}(s_0)}$$

$$\alpha \equiv A\frac{(E_F - P_{Fz})}{M_A} \simeq 1 - \frac{P_{Fz}}{m_p}$$

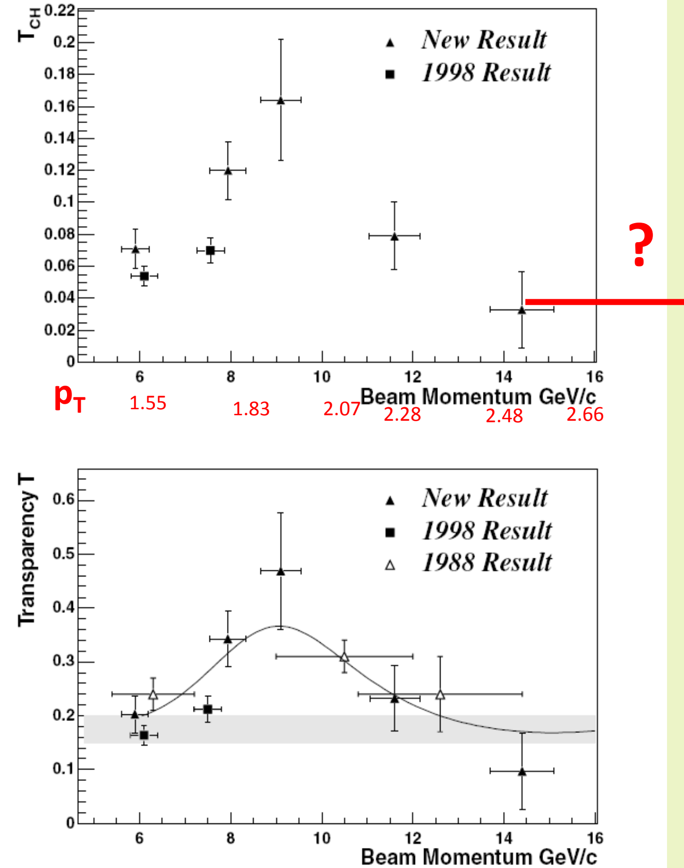

FIG. 2. Top: The transparency ratio $T_{\rm CH}$ as a function of the beam momentum for both the present result and two points from the 1998 publication [3]. Bottom: The transparency T versus beam momentum. The vertical errors shown here are all statistical errors, which dominate for these measurements. The horizontal errors reflect the α bin used. The shaded band represents the Glauber calculation for carbon [9]. The solid curve shows the shape R^{-1} as defined in the text. The 1998 data cover the c.m. angular region from 86°−90°. For the new data, a similar angular region is covered as is discussed in the text. The 1988 data cover 81°−90° c.m.

B.Van Overmeire, J.Ryckebusch, nucl-th/0608040

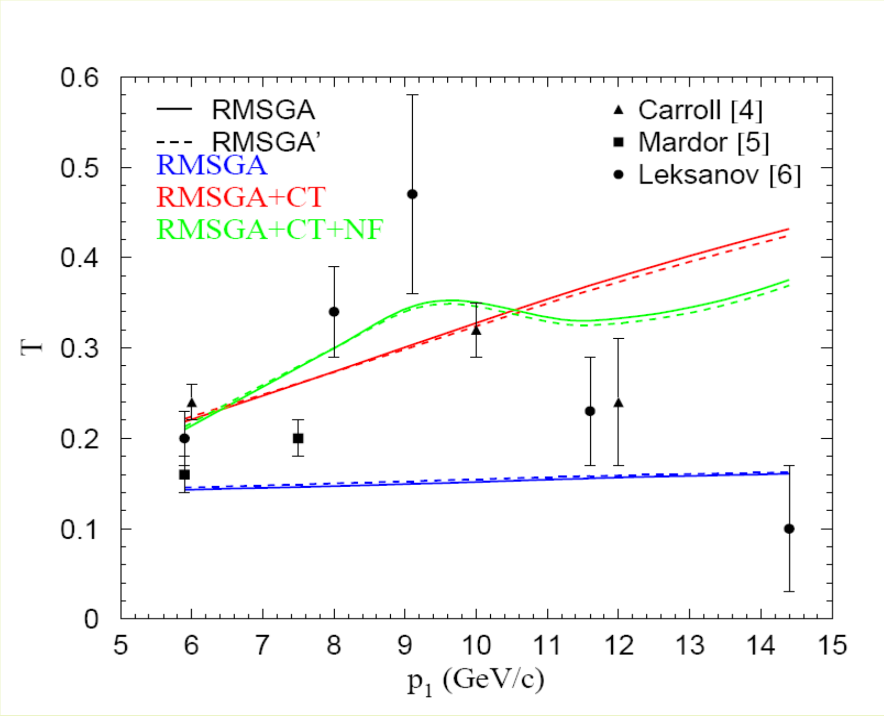

J. Aclander et al., Phys.Rev. C 70, 015208 (2004)

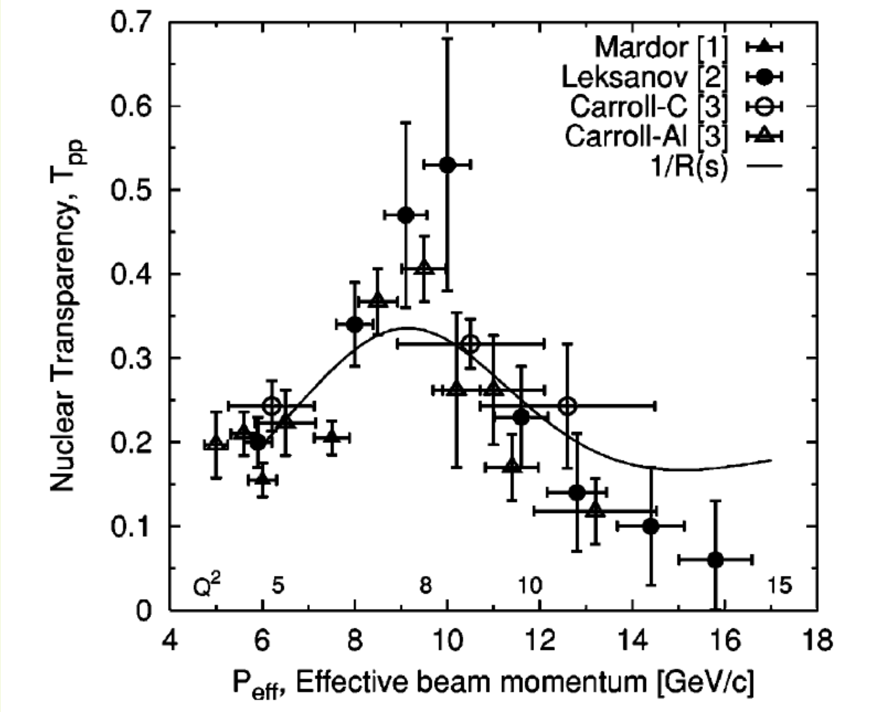

The Correlation Measurements

pA->h+X

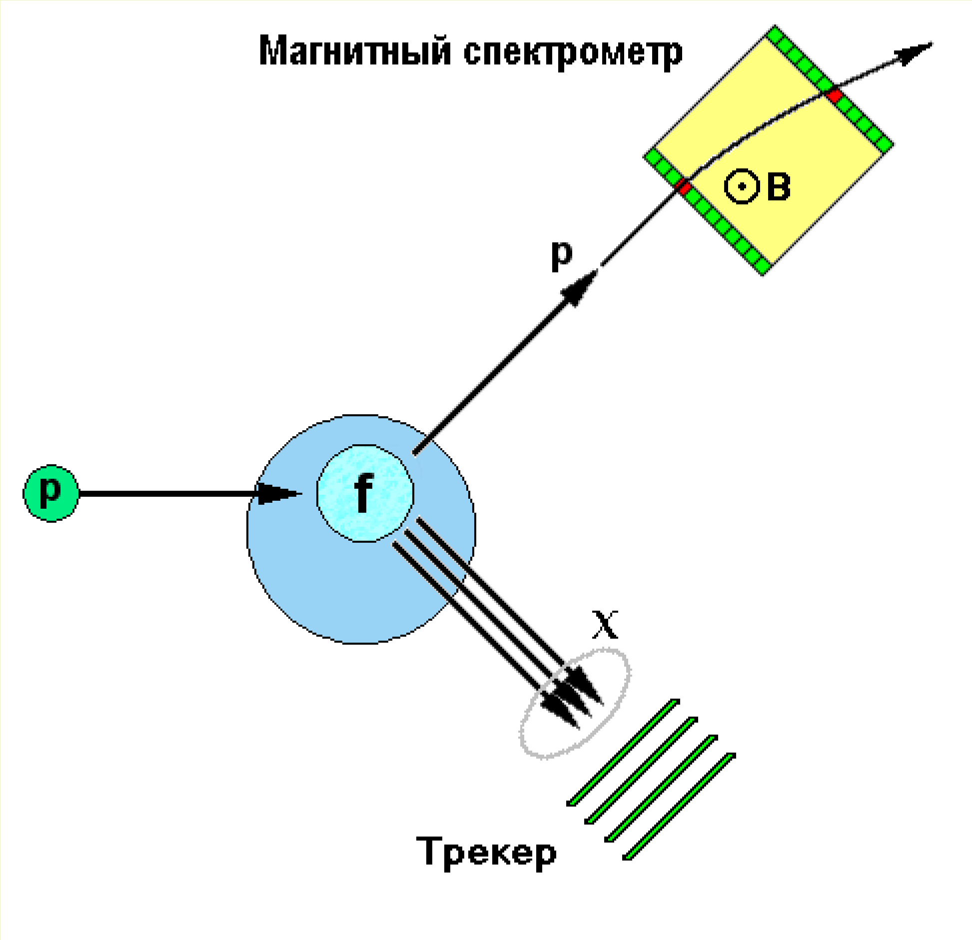

$x_T \sim 1$

FLINT, SPIN and FODS

FLINT@ITEP: $^{12}C + Be \to \gamma + X$

$\pi, \gamma, \gamma(\pi^o), \ldots$ high p_t

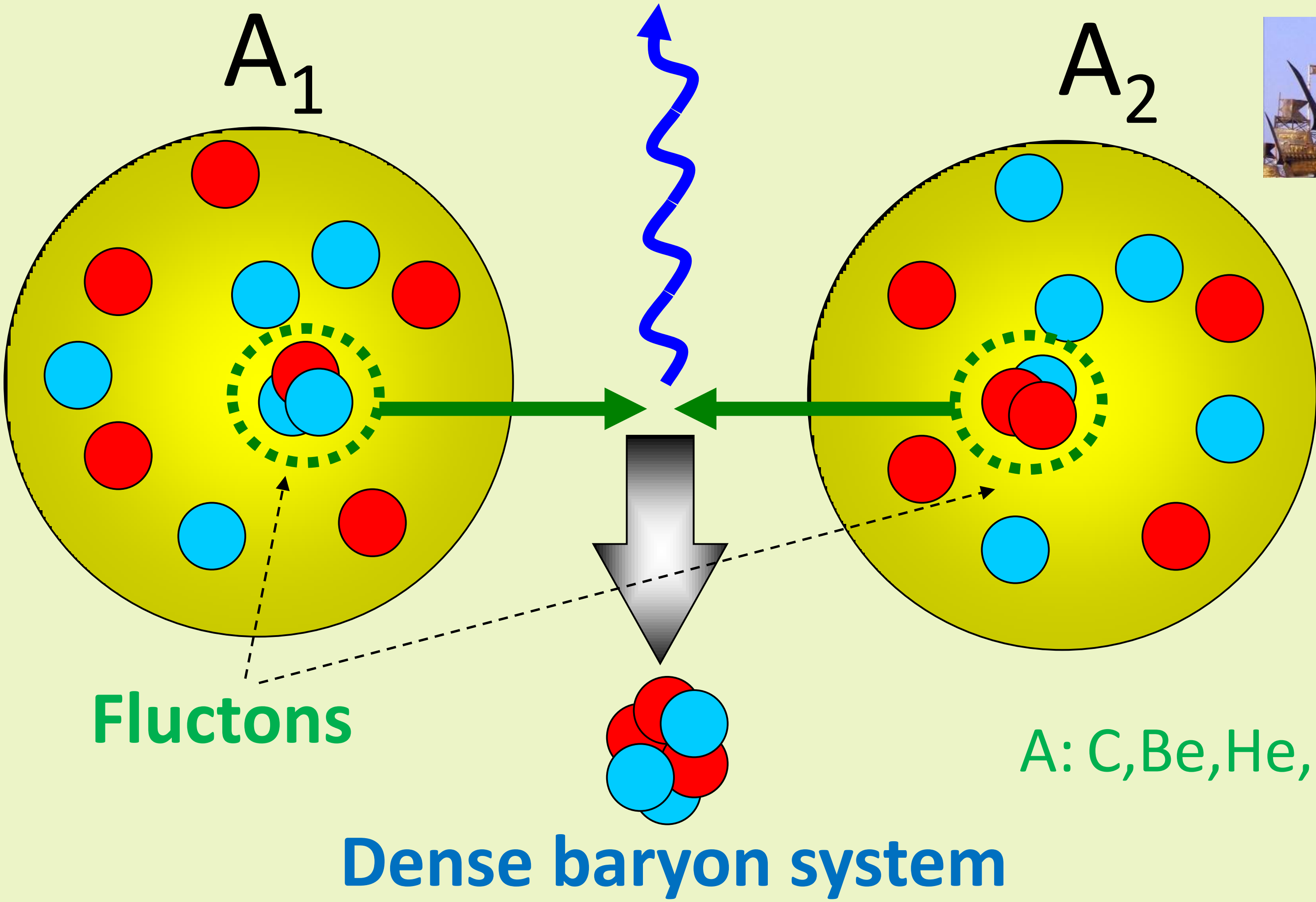

FLINT@ITEP: $^{12}C + Be \rightarrow \gamma + X$

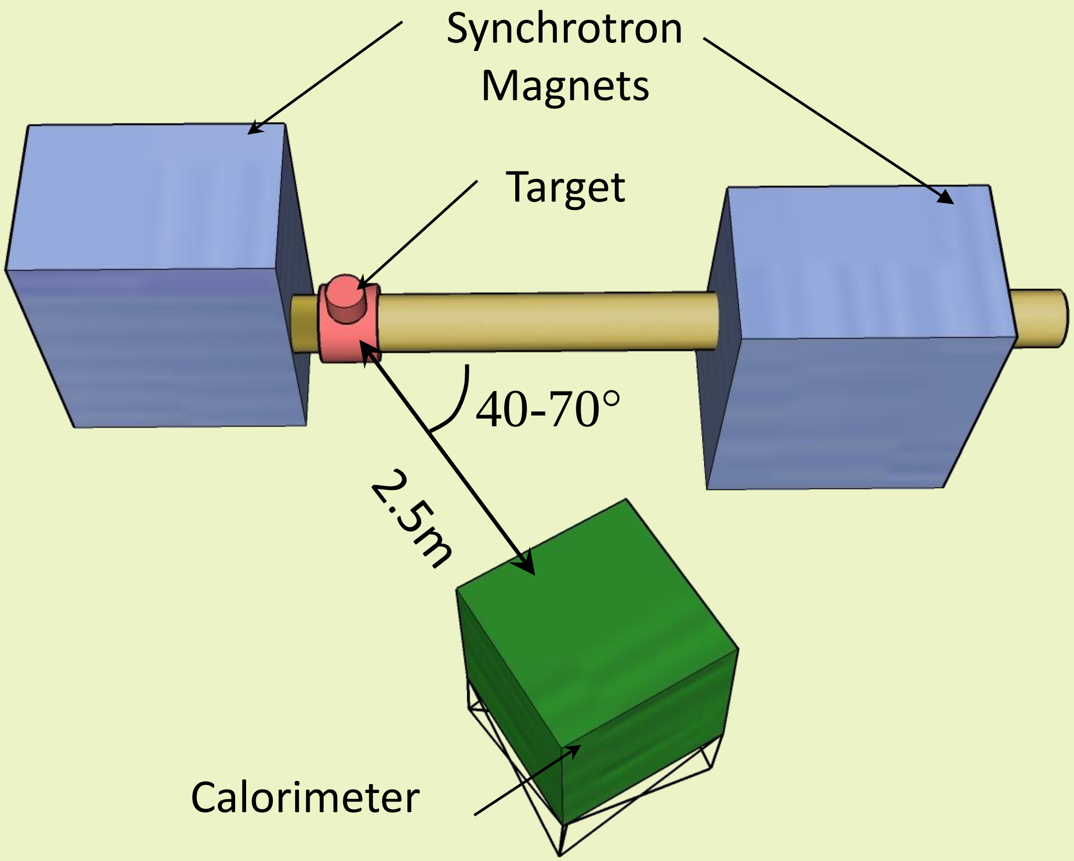

FLINT data

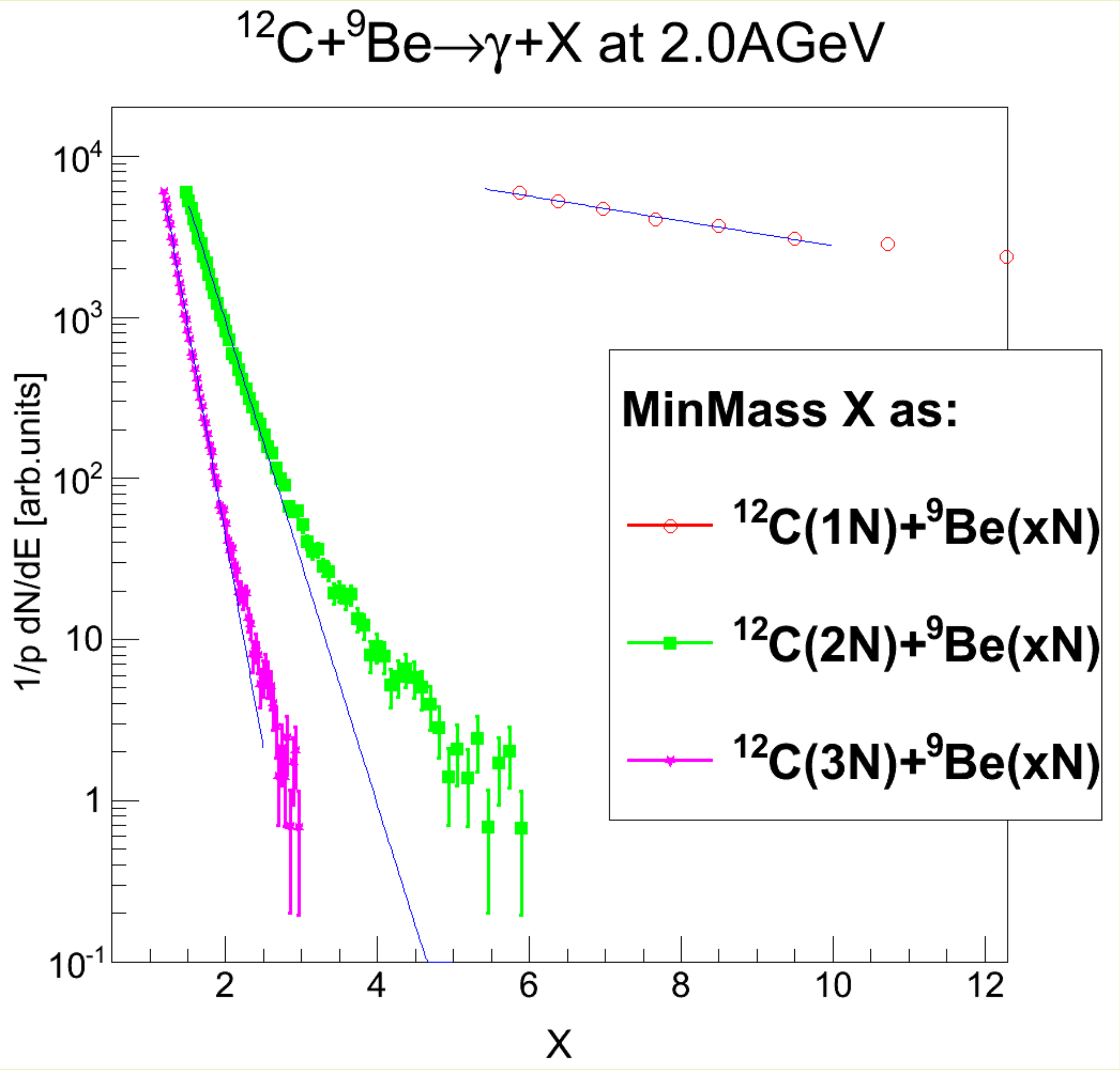

$^{12}C+^{9}Be\to\gamma+X$ at 2.0AGeV
1/p dN/dE [arb.units]
10^4
10^3
10^2
10
1
10^{-1}
2
4
6
8
10
12
X
MinMass X as:
$^{12}C(1N)+^{9}Be(xN)$
$^{12}C(2N)+^{9}Be(xN)$
$^{12}C(3N)+^{9}Be(xN)$

LAYOUT OF IHEP EXPERIMENTAL AREA

E=70 GeV,
I=1.7•10^{13} ppp
Beams of π, K, p, e, ν, A

- **Fast extraction**
- **Slow extraction**
- **Extraction by crystal**
- **Internal targets**

- Running experiments
- Experiments under preparation

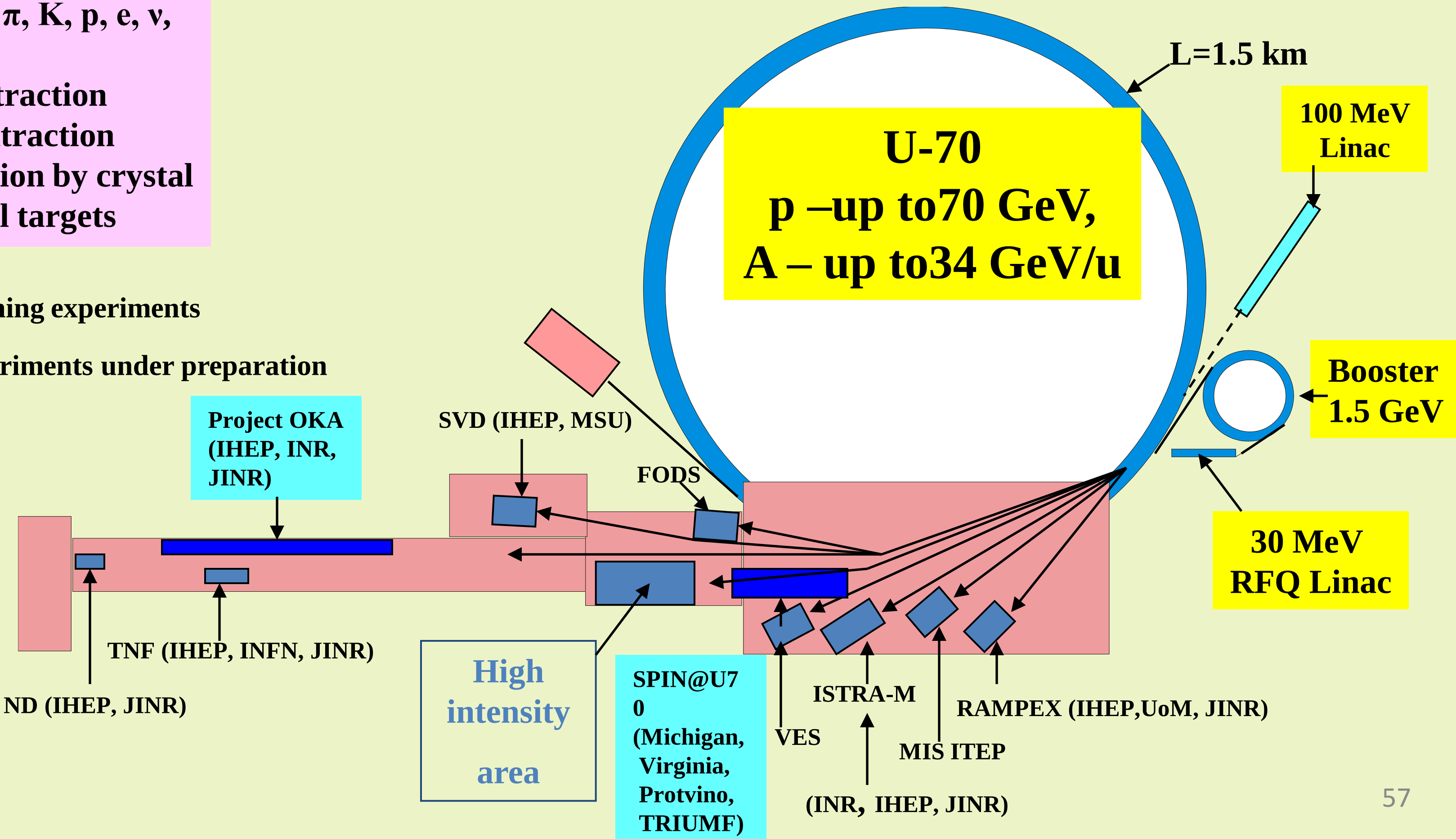

The current fixed target experiments at high p_T $(x_T \sim 1)$ region.

IHEP, Protvino

p up to 70 GeV

d, ^{12}C up to 34 GeV/u

The first SPIN data for cumulative particles (x>1) at $x_T \sim 1$.

$$p(50GeV) + A(C, Al, Cu, W) \rightarrow h^{+}(35^{0}\,Lab) + X$$

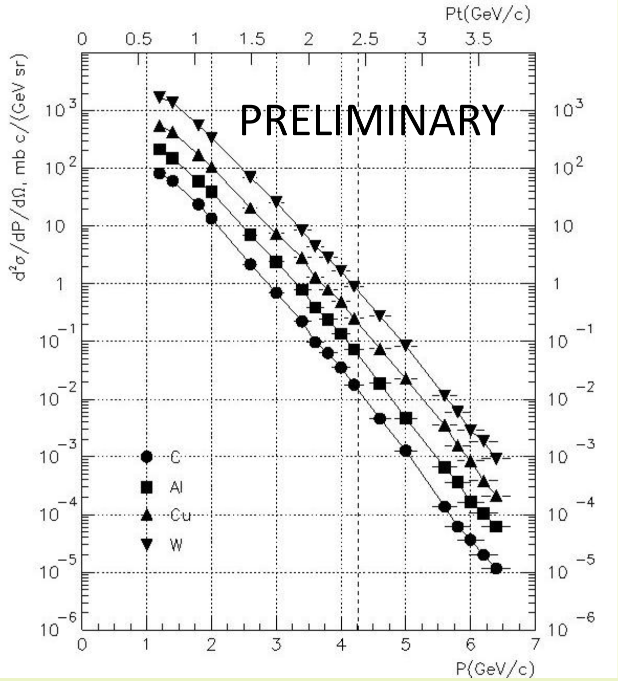

SPIN

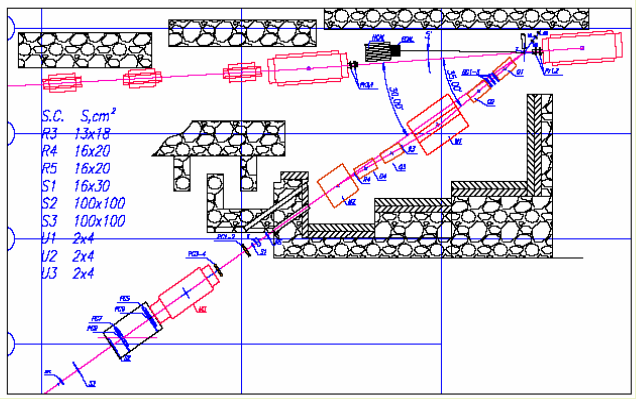

FODS

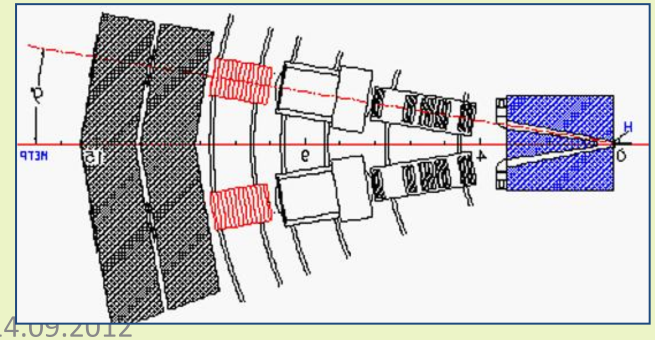

SPIN setup (IHEP, Protvino)

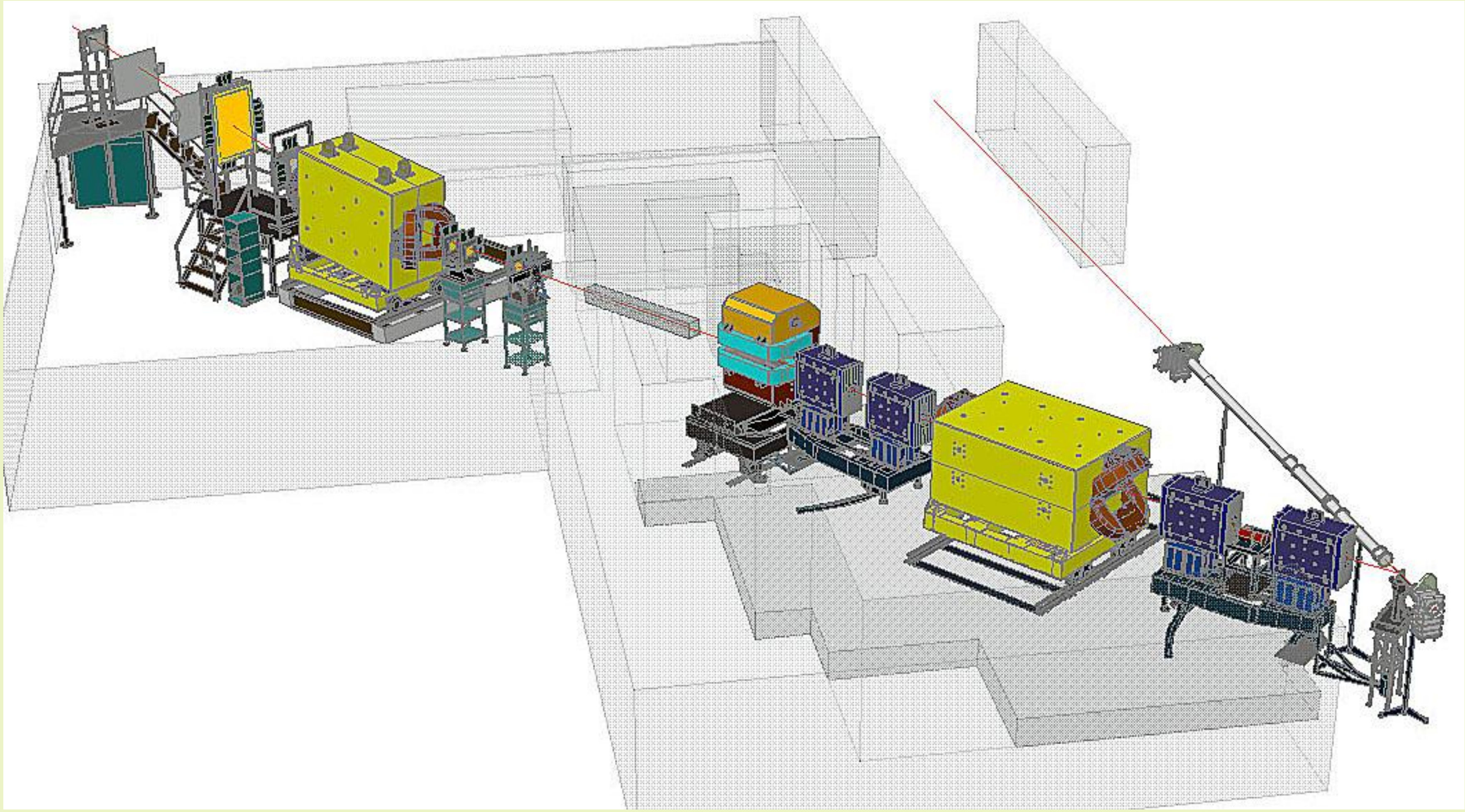

Target station

мишень	C	Al	Cu	W
Толщина(г/см2)	0.86	0.81	0.90	0.64

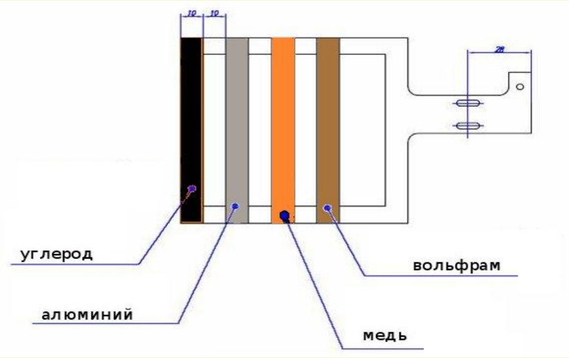

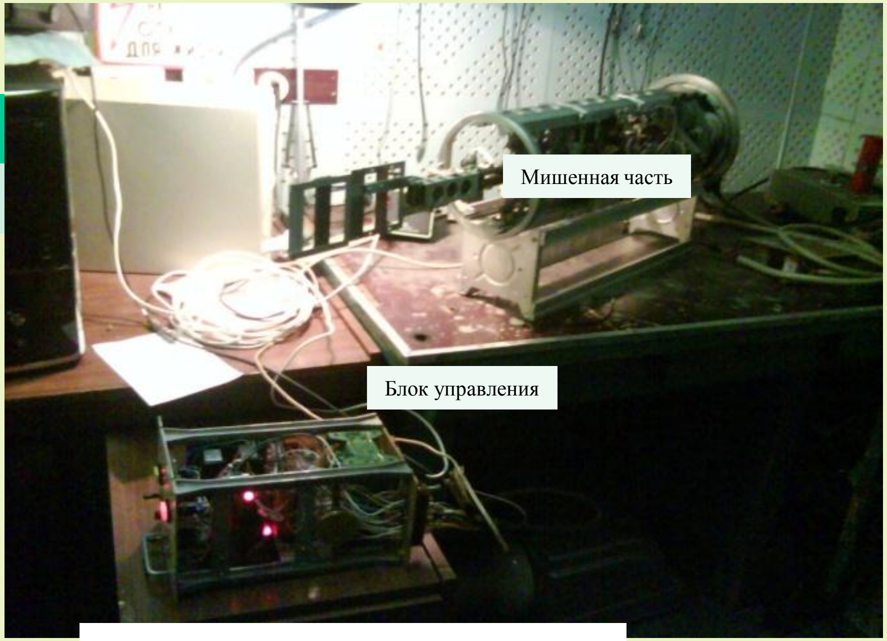

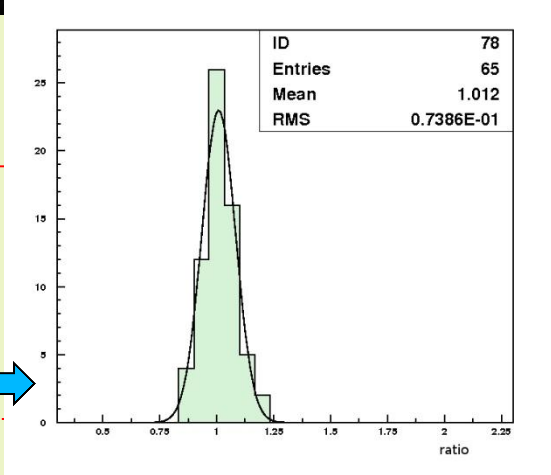

Мишени закреплены на одной рамке и вводятся в пучок поочередно, одна за одной. Так удается минимизировать систематику в измерении отношения выходов частиц на разных мишенях на уровне 7%

SPIN parameters

- **Registration angles $22^0 – 55^0$.** ***The first measurement for 35^0.***
- **Momentum resolution $\sigma(p)/p \approx 3\times10^{-3}$**
- **Azimuthal acceptance $\Delta\varphi \approx 100$ mrad, polar angle acceptance $\Delta\theta \approx 40$ mrad**
- **The setup capture for momentum changes from 5.5% at 1 GeV/c till 3.5% at 6 GeV/c.**
- **Beam intensity up to ~ 10^{13}.**
- **Accessible range of momentum at *35^0* :** ***P<6.6 GeV/c***

The first results have been presented at RAS session , ITEP,Nov. 24 2011

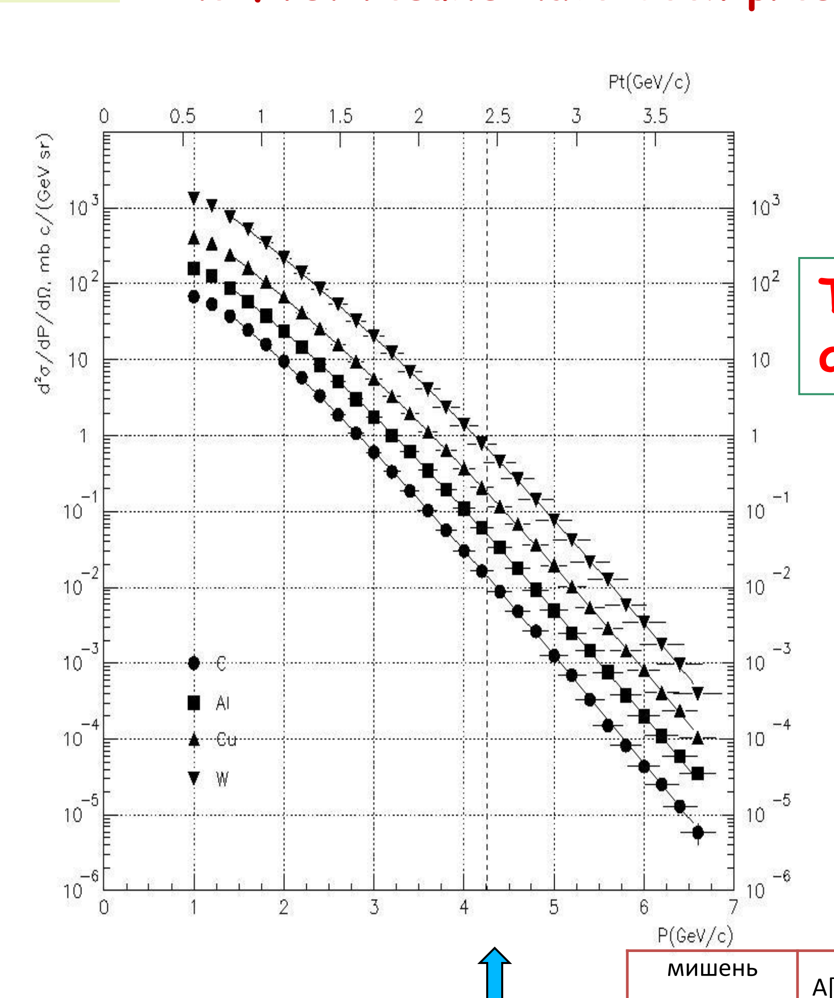

The first cumulative particle investigation at high p_T region, P_T> 2.5 ГэВ/c

$$\frac{d^2\sigma}{dPd\Omega} = \frac{A}{N_A \rho t} \cdot \frac{1}{\varepsilon \Delta P \Delta \Omega} \cdot \frac{1}{N_{prot}} \cdot N^{h+}$$

$$\frac{d^2\sigma}{dPd\Omega} = A \cdot \exp\left(B \cdot P + C \cdot P^2 + D \cdot P^3\right)$$

мишень	A[mb·c·GeV⁻¹·sr⁻¹]	B[c· GeV⁻¹]	C[c²· GeV⁻²]	D[c³ · GeV⁻³]
C	629.8±13.8	-1.626±0.012	-0.272±0.024	0.0146±0.0005
Al	1165.0± 84.9	-1.473 ±0.069	-0.266±0.021	0.0132±0.0019
Cu	3374.8±190.9	-1.612 ±0.056	-0.191± 0.016	0.0059±0.0014
W	10290.0±1116.8	-1.604+0.102	-0.171±0.029	0.0040±0.0025

Kinematical limit for elastic NN scattering

Comparisons MC with SPIN data

Solid lines: HIJING 1.3 http://www-nsdth.lbl.gov/~xnwang/hijing/doc.html
Dot lines: UrQMD 3.3 http://urqmd.org/

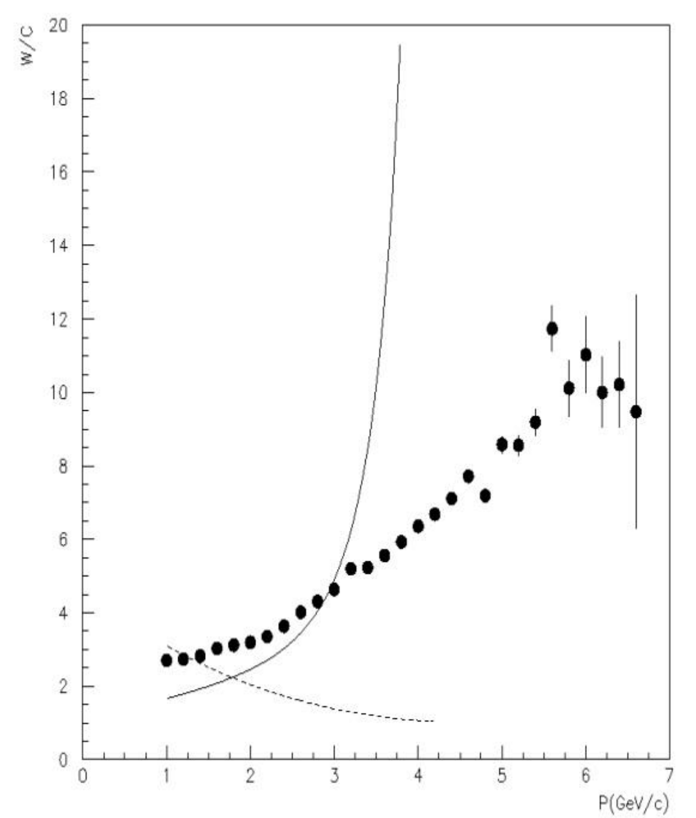

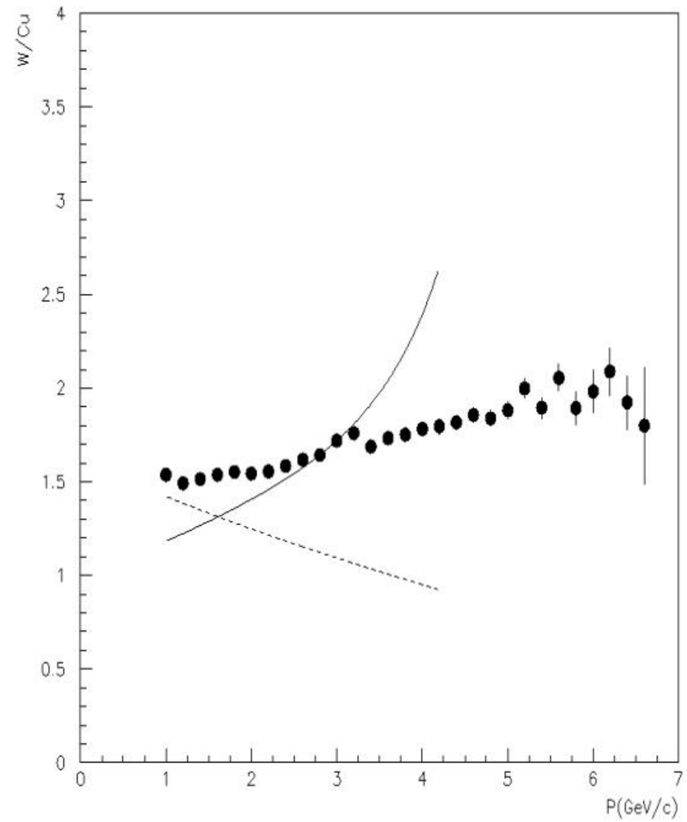

A-dependence

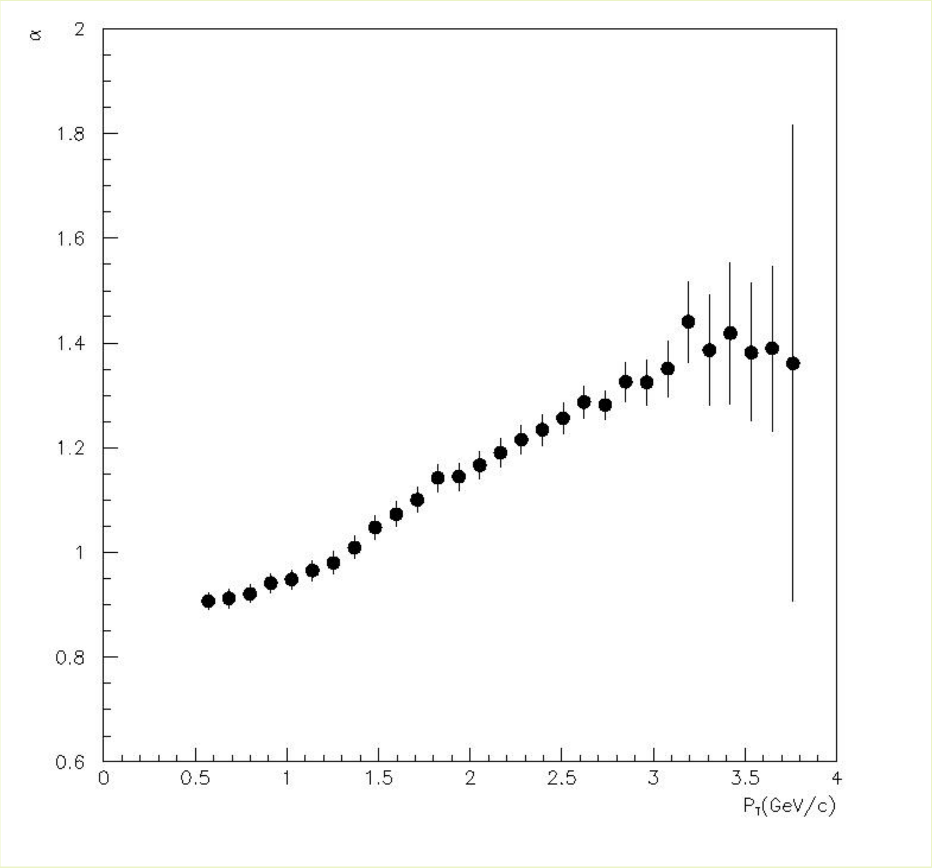

$$\sigma \sim A^{\alpha}$$

$$\alpha = \ln\left(\frac{\sigma_w}{\sigma_c}\right) / \ln\left(\frac{A_w}{A_c}\right)$$

We deal with multinucleon configuration, but local this interaction?

Local processes in NN kinematic

ИЗМЕРЕНИЕ СЕЧЕНИЙ ОБРАЗОВАНИЯ АДРОНОВ С ИМПУЛЬСОМ ДО 2 ГэВ/*c* В ПРОТОН-ЯДЕРНЫХ СТОЛКНОВЕНИЯХ ПРИ 70 ГэВ

БАРКОВ Л. М., ЗОЛОТОРЁВ М. С., КОТОВ В. И. [1], ЛЕБЕДЕВ П. К., МАКАРЬИНА Л. А. [2], МИШАКОВА А. П. [2], ОХАПКИН В. С., РЗАЕВ Р. А. [1], САХАРОВ В. П. [1], СМАХТИН В. П., ШИМАНСКИЙ С. С.

ИНСТИТУТ ЯДЕРНОЙ ФИЗИКИ СО АН СССР

(Поступила в редакцию 2 августа 1982 г.)

ЯДЕРНАЯ ФИЗИКА
JOURNAL OF NUCLEAR PHYSICS
т. 37, вып. 5, 1983

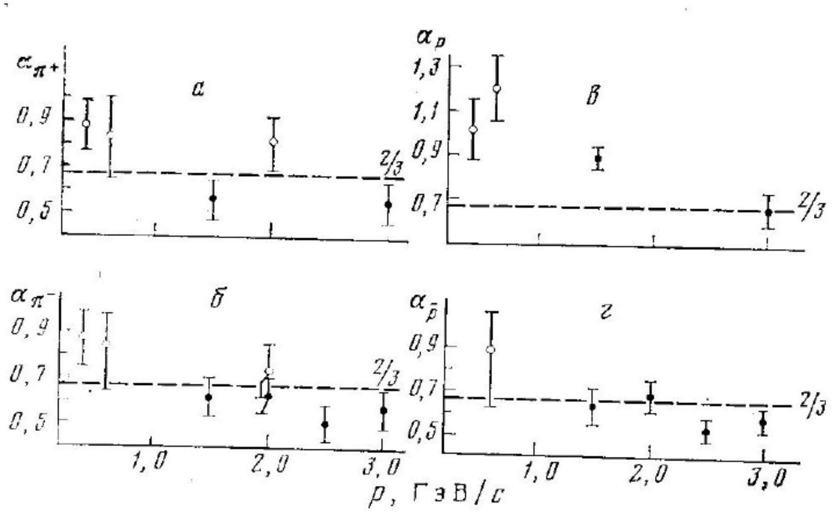

Рис. 4. Зависимость показателя α от импульса для положительных пионов (*а*), отрицательных пионов (*б*), протонов (*в*) и антипротонов (*г*) (● – [11], ○ – данная работа)

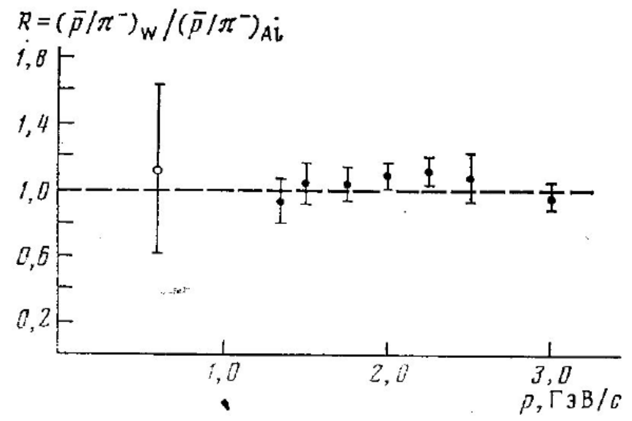

Рис. 6. Сравнение отношений выходов антипротонов и отрицательных пионов для W и Al мишеней в зависимости от импульса частиц (● – [11], ○ – данная работа)

p/π ration

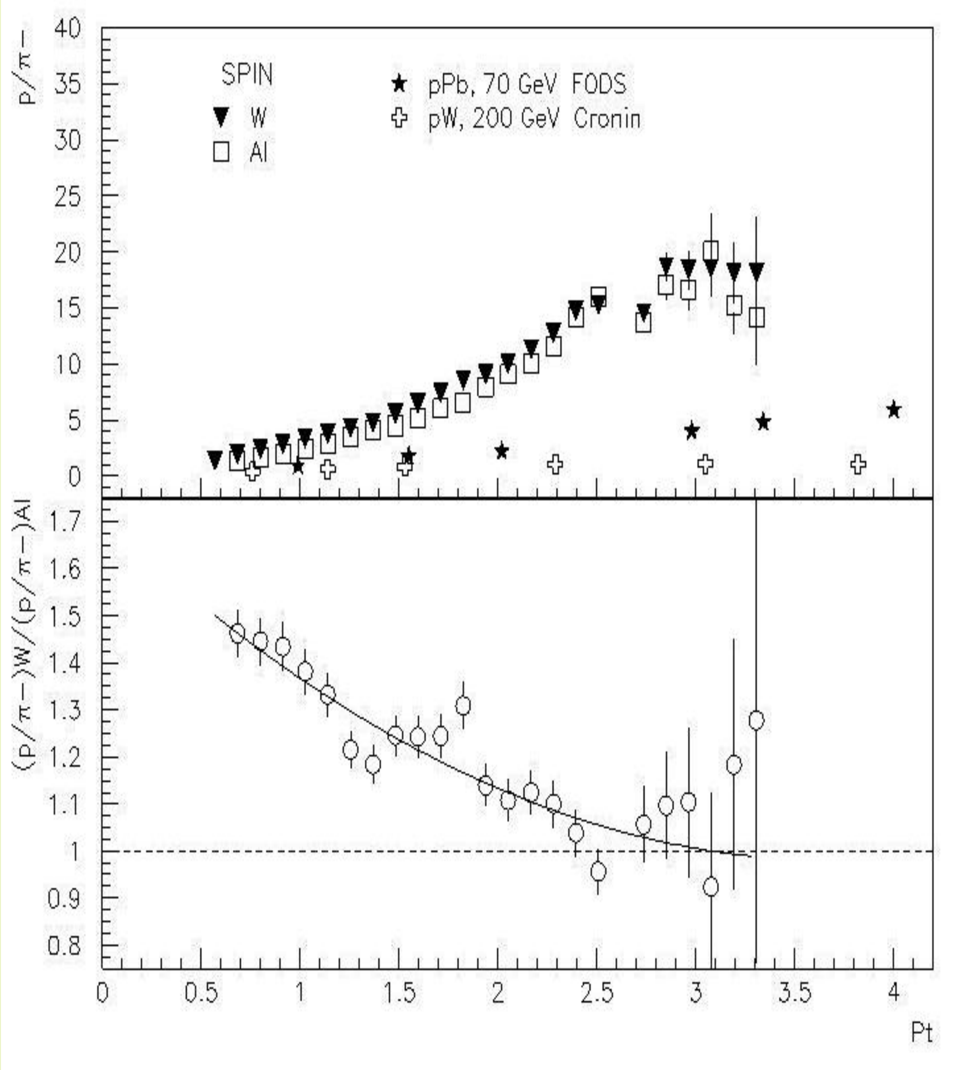

- С ростом поперечного импульса наблюдается значительно больший выход протонов по отношению к пионам.

- Отсутствие зависимости p/π⁻ от атомного числа при больших Pt может рассматриваться как указанием на локальный механизм образования частиц и малый вклад процессов вторичного взаимодействия

FODS: В.В. Абрамов и др., ЯФ, т.41, вып.2, 357-370(1985)

Cronin: D. Antreasyan et al.,Phys. Rev. D 19, 764–778 (1979).

SPIN(IHEP, protvino)
p+A->h +X (35^0 lab system), with 50 GeV proton beam

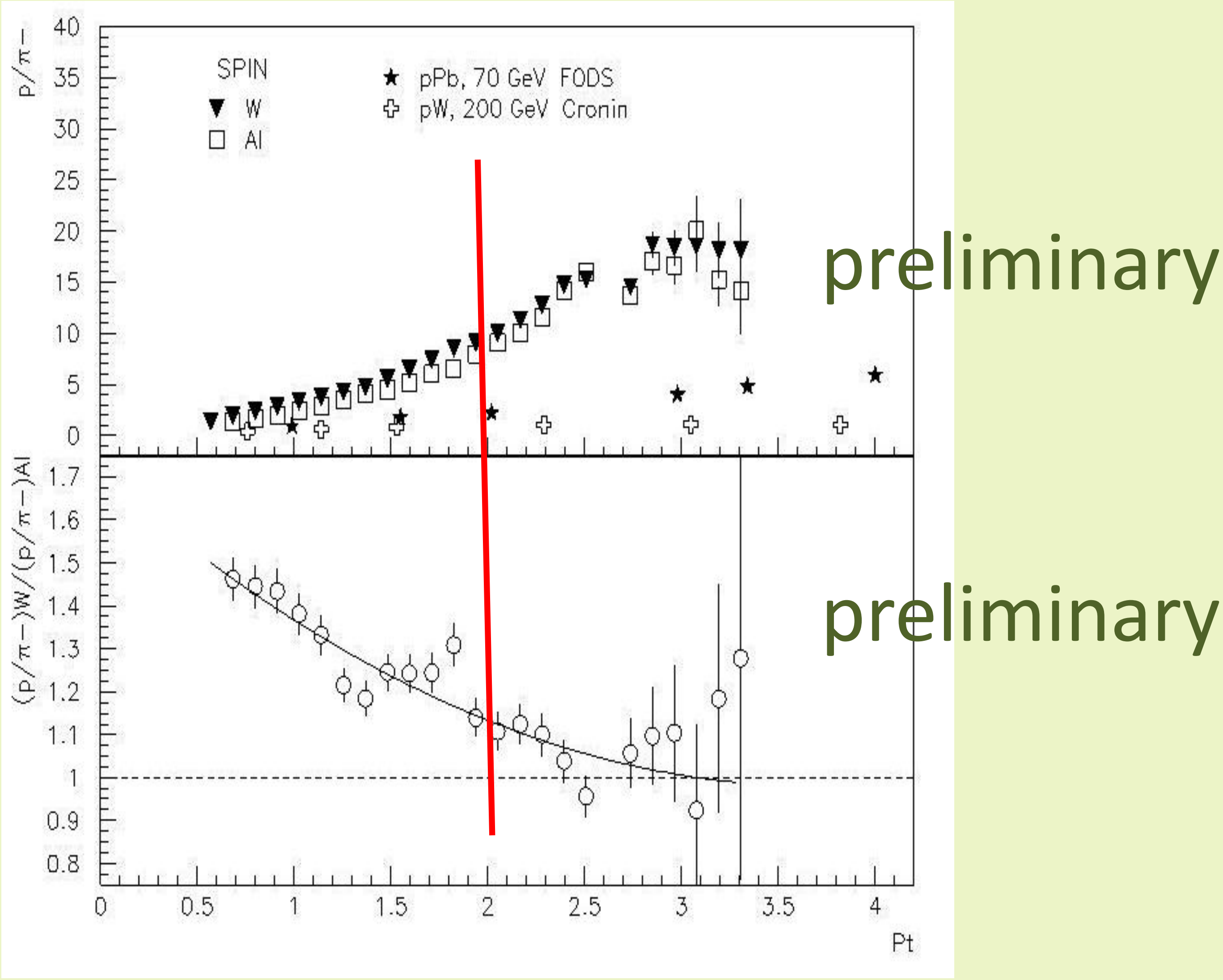

FODS: В.В. Абрамов и др., ЯФ, т.41, вып.2, 357-370(1985)

Cronin: D. Antreasyan et al.,Phys. Rev. D 19, 764–778 (1979).

Cumulative A-dependence:

$$\frac{f_{A_{II}^{1}}}{f_{A_{II}^{2}}} \sim \left(\frac{A_{II}^{1}}{A_{II}^{2}}\right)^{\left(\frac{1}{3}+\frac{X_{II}}{3}\right)}$$

Откуда следует, что отношение сечений, умноженное на обратную A-зависимость должно быть близко к константе.

протоны

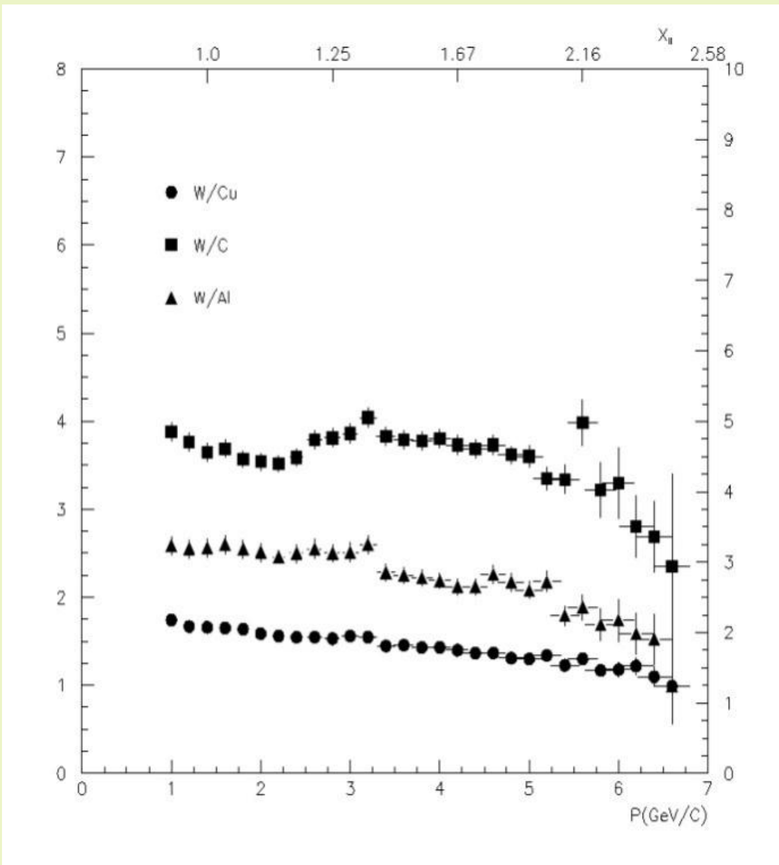

отрицательные пионы

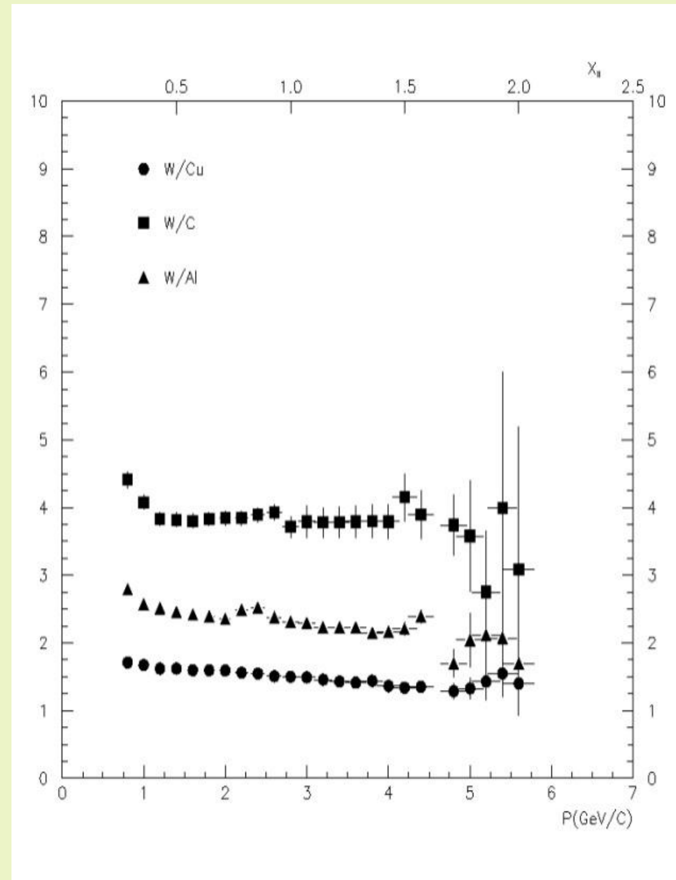

Flucton fragmentation – same side flow

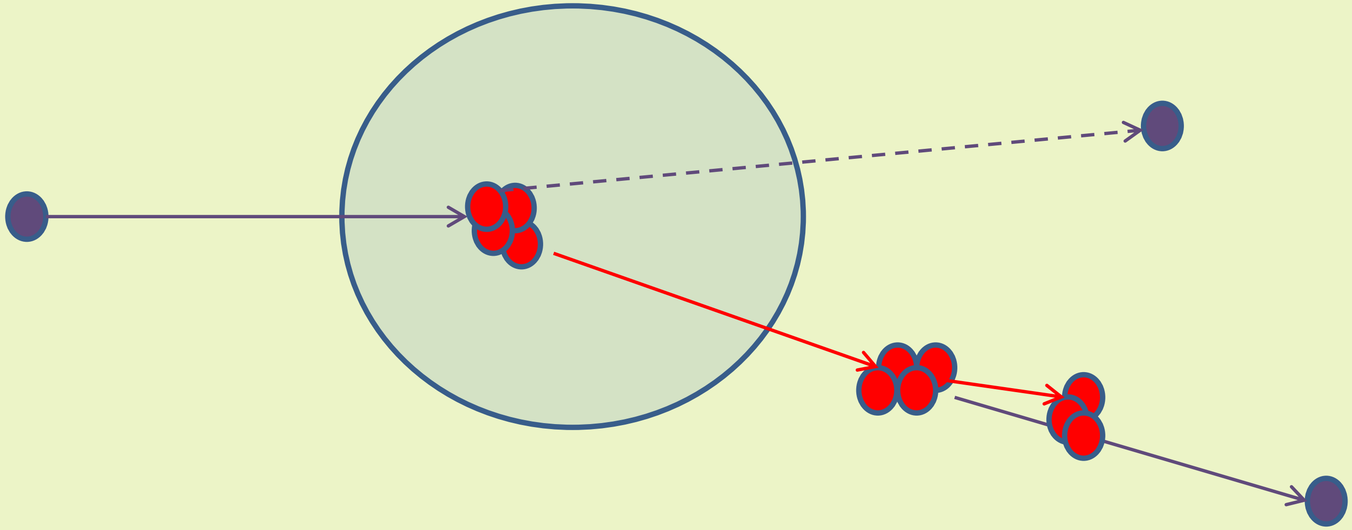

ГОСУДАРСТВЕННЫЙ НАУЧНЫЙ ЦЕНТР РОССИЙСКОЙ ФЕДЕРАЦИИ

ИНСТИТУТ ФИЗИКИ ВЫСОКИХ ЭНЕРГИЙ

FODS (IHEP, Protvino)

$pp, pA, AA - \text{interactions}$

1.4. Исследования эффектов цветовой (ядерной) прозрачности

ИФВЭ 2011–32
ОЭФ

1.5. Аномалия при $p_T \sim 2$ ГэВ/c

А.А. Балдин[1], Я.А. Бердников[2], А.И. Берлёв[1], А.Ю. Бордановский, Ю.Т. Борзунов[1], А.А. Волков, В.П. Ефремов, А.Е. Иванов[2], А.Ю. Калинин, В.Т. Ким[2,3], А.В. Константинов[1], А.В. Кораблёв, В.И. Корешев, А.Н. Криницын, В.И. Крышкин, И.В. Кудашкин[1], Н.В. Кулагин, А.А. Логинов, В.А. Мурзин[3], В.А. Орешкин[3], Е.Б. Плеханов[1], В.В. Скворцов, В.В. Талов, Л.К. Турчанович, С.С. Шиманский[1]

$$\pi + p \to \pi\pi(\pi p)$$

$$p + p \to \pi\pi(\pi p, pp)$$

Программа корреляционных исследований при взаимодействии адронов и ядер при больших x_T

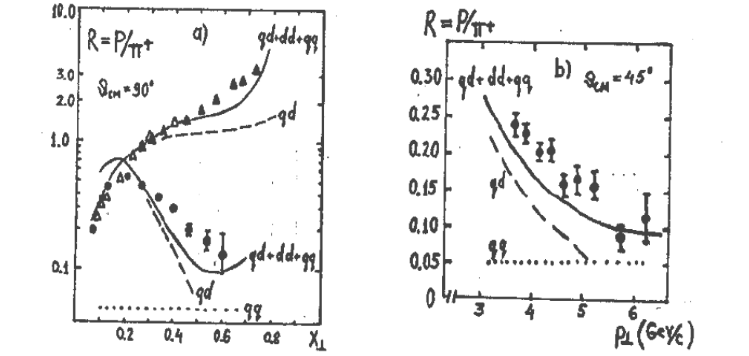

Рис. 9. Отношение $R=p/\pi^+$ в pp-взаимодействиях: а) при $\theta_{см}=90^0$: • – данные ФНАЛ при $\sqrt{s}$=23,4 ГэВ, Δ, ▲ – данные ФОДС для $\sqrt{s}$=11,5 ГэВ; b) $\theta_{см}=45^0$: • – данные ISR при $\sqrt{s}$=62 ГэВ.

[1]ОИЯИ, Дубна
[2]СПбГПУ, Санкт-Петербург
[3]ПИЯФ, Гатчина

Протвино 2011

THE END

The Highest Energy
RHIC and LHC

pp -> π + X

PHYSICAL REVIEW D **76**, 051106(R) (2007)

Inclusive cross section and double helicity asymmetry for π^0 production in $p + p$ collisions at $\sqrt{s} = 200$ GeV: Implications for the polarized gluon distribution in the proton

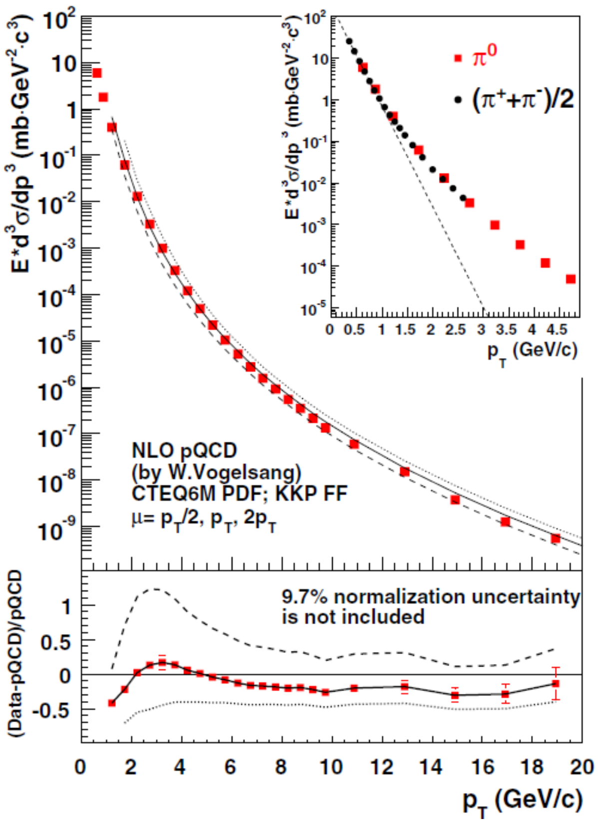

for higher p_T. This is the basis for applying the pQCD formalism to the double helicity asymmetry data with $p_T > 2$ GeV$/c$.

PHYSICAL REVIEW D **79**, 012003 (2009)

Inclusive cross section and double helicity asymmetry for π^0 production in $p + p$ collisions at $\sqrt{s} = 62.4$ GeV

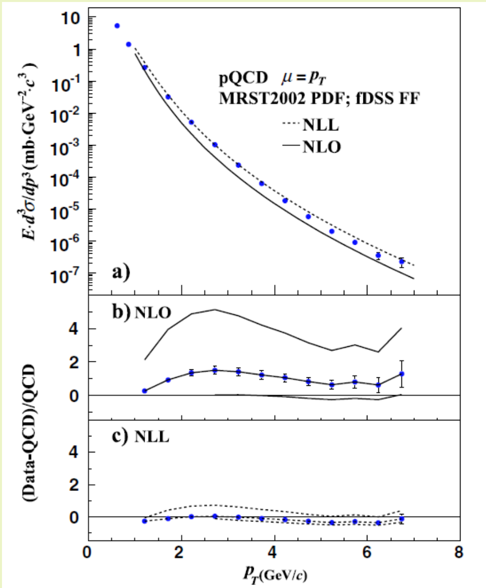

Fig. 4(b). A similar drop in the parameter n at $x_T \gtrsim 0.1$ was observed at ISR energies [12]. Figure 4(b) also shows the possible transition from soft- to hard-scattering regions in π^0 production at $p_T \sim 2$ GeV$/c$. A similar conclusion was derived from the shape of the π^0 spectrum at $\sqrt{s} = 200$ GeV in [5]. This can serve as a basis for applying the pQCD formalism to the double helicity asymmetry data with $p_T > 2$ GeV$/c$ in order to allow access to ΔG.

The nuclear modification factor at RHIC and LHC

- quantify departure from binary scaling in AA

→ ratio of yield in AA versus reference collisions

- e.g.: reference is pp → R_{AA}

$$R_{\mathrm{AA}} = \frac{\mathrm{Yield}_{\mathrm{AA}}}{\mathrm{Yield}_{\mathrm{pp}}} \cdot \frac{1}{\langle Nbin \rangle_{\mathrm{AA}}}$$

- …or peripheral AA → Rcp ("central to peripheral")

$$R_{\mathrm{cp}} = \frac{\mathrm{Yield}_{\mathrm{AA,\,central}}}{\mathrm{Yield}_{\mathrm{AA,\,periph}}} \cdot \frac{\langle Nbin \rangle_{\mathrm{AA,periph}}}{\langle Nbin \rangle_{\mathrm{AA,\,central}}}$$

high p_t suppression seen by all experiments

R_{AA}=yield(AuAu)/N_{coll} yield(pp)

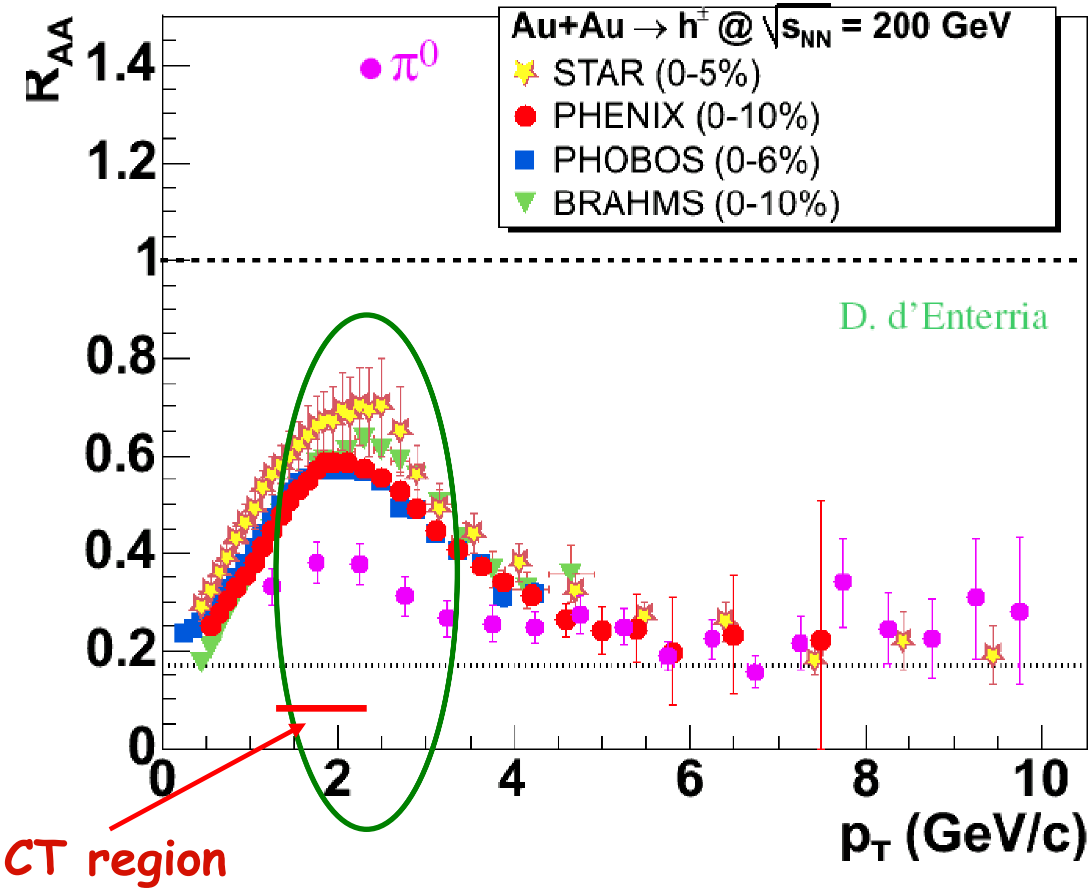

- ⋆ all expts. see large suppression in AuAu
- ⋆ π^0 lower than $h^{\pm}$
- ⋆ no suppression in dAu rather Cronin enhancement → medium effect, not incoming partons

- ➔ reasonable agreement between 4 experiments

p_T~2 GeV/c anomaly at high energy (RHIC and LHC)

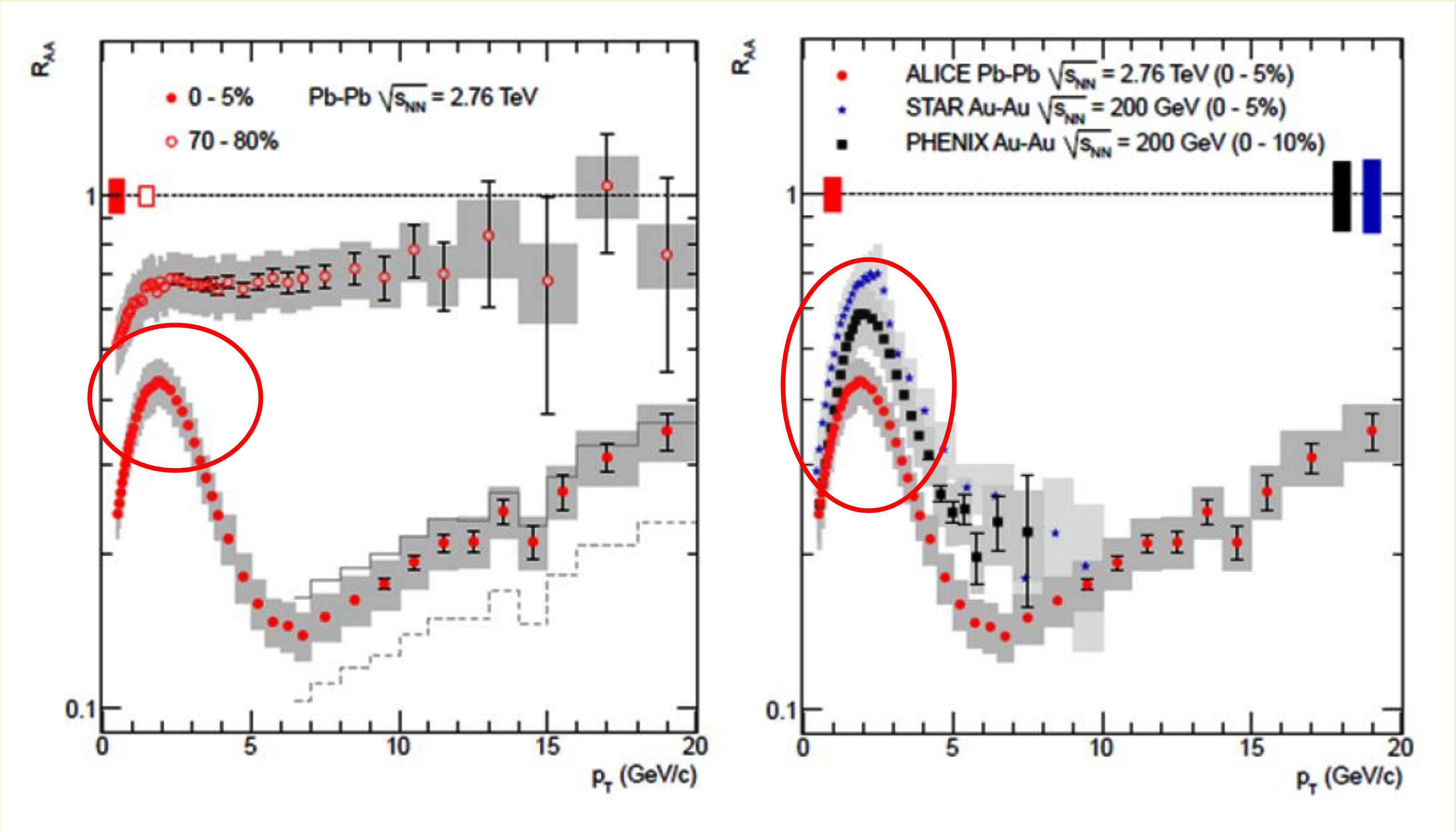

J.W. Cronin et al., Production of hadrons at large transverse momentum at 200, 300, and 400 GeV, Phys.Rev. D, v.11, N 11, 3105-3123 (1975)

p_T ~ 2 GeV/c region

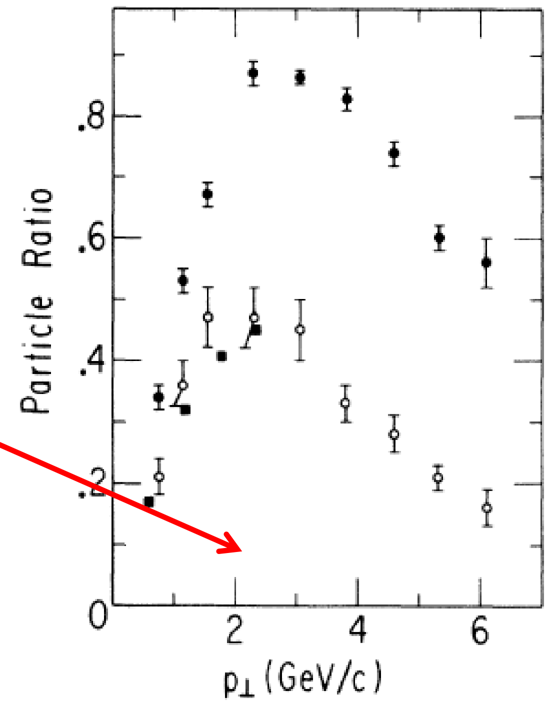

FIG. 20. Comparison of the cross-section ratio p/π^+ measured on tungsten at $\sqrt{s}=23.7$ GeV (closed circles), with that obtained by extrapolation to $A=1$ (open circles). Ratios obtained from the British-Scandinavian collabortion (Ref. 23) at $\sqrt{s}=23.4$ GeV are also plotted (closed squares).

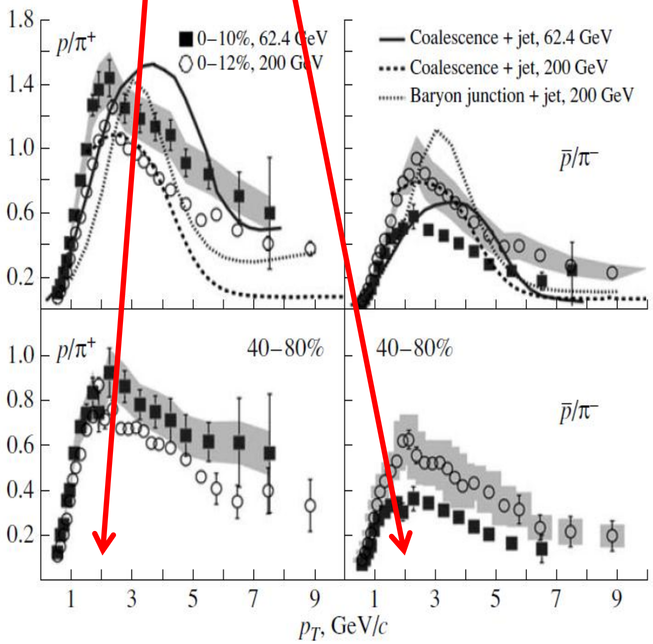

Fig. 3. [10] Ratio of the cross sections for the production of protons and charged pions as a function of the transverse momentum for various degrees of centrality and two beam energies of 62.4 and 200 GeV: (points) results of the STAR experiment and (curves) results of model calculations.

V.S. Pantuev *Physics of Atomic Nuclei, 2009, Vol. 72, No. 12, pp. 1971–1981*